



1 Implementation of regenerative ditch borders in Dutch  
2 peat meadows: effects on soil CO<sub>2</sub> fluxes and potential  
3 carbon trade-offs

4

5 **Authors**

6 Sanne E. Bethe<sup>1</sup>, Mariet M. Hefting<sup>1</sup>, Joao R. Wendrich Teixeira<sup>1</sup>, Matty P. Berg<sup>2,3</sup> and James  
7 T. Weedon<sup>1</sup>

8

9 **Affiliations**

10 <sup>1</sup>Section Systems Ecology, Amsterdam Institute for Life and Environment, Vrije  
11 Universiteit, Amsterdam, The Netherlands, <sup>2</sup>Section Ecology and Evolution, Amsterdam  
12 Institute for Life and Environment, Vrije Universiteit, Amsterdam, The Netherlands,  
13 <sup>3</sup>Groningen Institute for Evolutionary Life Sciences, Community and Conservation  
14 Ecology Group, University of Groningen, Groningen, The Netherlands.

15

16 **Article type:** research article

17

18 **Corresponding author address:** Sanne E. Bethe, section Systems Ecology, Amsterdam  
19 Institute for Life and Environment, Vrije Universiteit Amsterdam, De Boelelaan 1108  
20 1081HZ Amsterdam, the Netherlands

21 **Email:** s.e.bethe@vu.nl

22 **Phone:** +31614391811

23 **ORCID iD:** 0000-0002-5597-617X

24



25 **Abstract**

26 Drained peatlands account for 3 % of the Dutch national greenhouse gas (GHG)  
27 emissions. Topsoil removal (TSR; which leads to removal of built-up nutrients and labile  
28 soil carbon) in combination with rewetting (groundwater table management) in drained  
29 peatlands is often proposed as a restoration measure effective in reducing carbon  
30 dioxide (CO<sub>2</sub>) emissions, yet often politically challenging to implement. TSR is however  
31 currently applied at a smaller scale during the implementation of regenerative ditch  
32 borders (RDBs), but its effectiveness in reducing CO<sub>2</sub> remains uncertain. We investigated  
33 the effects of RDBs on soil CO<sub>2</sub> emissions in comparison to conventional borders (CDBs)  
34 in a year-round field survey (June 2023 – March 2024) in a lowland peat agroecosystem.  
35 Soil respiration was measured at four distances from the water's edge (40, 80, 360 and  
36 640 cm) over a ten-month period and used to fit statistical models with the predictors soil  
37 temperature, soil moisture content and exposed carbon (a variable integrating profile soil  
38 carbon density and groundwater level). The resulting model was used to calculate annual  
39 soil respiration, and to estimate the payback time (no. of years for net negative effects on  
40 cumulative CO<sub>2</sub> emissions) of the removed carbon. Spatiotemporal variation in soil  
41 respiration was mostly explained by exposed carbon and soil temperature (32 % and 30  
42 %, respectively). Soil respiration peaked at 65 % soil moisture content. At distances 40  
43 and 80 cm reduced soil respiration in RDBs in spring and summer was driven by lower  
44 amounts of exposed carbon, while at 360 and 640 cm in RDBs higher soil temperatures  
45 and soil moisture content mostly counteracted this effect. Model-based annual soil  
46 respiration was 17 % lower in RDBs in comparison to CDBs. If it is assumed that all soil  
47 carbon removed during RDB construction is mineralized, the payback time can exceed  
48 100 years. While RDBs can promote reductions in soil CO<sub>2</sub> emissions and therefore more  
49 sustainable peatland-adapted agriculture, potential emissions from excavated carbon  
50 should be accounted for.

51



## 52 1 Introduction

53 Globally peatlands function as an important carbon stock. They cover only 3 % of the  
54 world's land surface, yet store an estimated 547 Gt of carbon, predominantly in  
55 peatlands located in the Northern Hemisphere (Yu et al., 2010). In peat ecosystems, high  
56 water tables create anoxic conditions which have facilitated organic matter  
57 accumulation since the Last Glacial Maximum (Gorham, 1991; Yu et al., 2010; Leifeld &  
58 Menichetti, 2018). Over the last decades, human-induced land use changes - most  
59 importantly land reclamation for agricultural purposes, or mining of peat for fuel - have  
60 significantly impacted peatlands, threatening their status as carbon sinks (Joosten, 2009;  
61 Tanneberger et al., 2021). Currently, over 65 million ha of peat soils are classified as  
62 degraded, with drainage being the main driver (Joosten, 2015). In Northwest Europe,  
63 peatlands have been drained for agricultural purposes for centuries to allow cattle and  
64 heavy machinery on the land, and to ensure high grassland productivity (van de Ven,  
65 1993; Wereld Natuur Fonds, 2020). However, drainage enables oxygen intrusion into the  
66 soil, which enhances aerobic microbial decomposition rates in the unsaturated peat  
67 zone, and therefore increases CO<sub>2</sub> emissions into the atmosphere and induces land  
68 subsidence (Brouns et al., 2014; Erkens et al., 2016; Joosten, 2009). Ongoing processes  
69 of peat degradation therefore have major implications for the soil carbon cycle, resulting  
70 in calls for peatland management actions that minimize or reverse the negative  
71 consequence of human activity (Chimner et al., 2017; Humpenöder et al., 2020; Zak &  
72 McInnes, 2022). Improving our process understanding and prediction accuracy of CO<sub>2</sub>  
73 emissions from drained peatlands is important for accurate carbon accounting and  
74 assessment of the carbon-cycle impact of these proposed management measures.

75 In peat soils the key process driving soil CO<sub>2</sub> emissions is microbe-mediated enzymatic  
76 breakdown of organic matter which is mostly driven by reaction kinetics, availability of  
77 electron acceptors and the biochemical composition of the substrate (Findlay, 2021).  
78 Environmental condition affect the reaction kinetics of soil carbon decomposition, with  
79 increasing soil temperatures causing exponentially increasing soil CO<sub>2</sub> emissions due to  
80 enhanced microbial activity and reaction rates (Davidson & Janssens, 2006; Kucera &  
81 Kirkham, 1971). Oxygen is the electron acceptor in the process of aerobic peat



82 decomposition, and its availability in the soil therefore strongly determines peat  
83 oxidation and soil CO<sub>2</sub> emissions (Boonman et al., 2024). The biogeochemical quality of  
84 the substrate is mostly driven by the chemical composition of the litter of the main peat-  
85 building plant species (e.g. *Alnus glutinosa*, *Carex* spp., *Phragmites australis*, or  
86 *Sphagnum* spp. in temperate and boreal-zone peatlands), which can influence inherent  
87 decomposition rates (Tolunay et al., 2024). These pore-scale processes can be translated  
88 into field-scale drivers of soil CO<sub>2</sub> emissions, such as soil moisture content, water table  
89 depth, carbon availability and seasonality. When soil moisture content is low it limits the  
90 supply of substrates and creates osmotic stress for soil microbes and when soil moisture  
91 is high the diffusion of oxygen becomes limited (Skopp et al., 1990; Schjønning et al.,  
92 2003; Manzoni et al., 2012; Moyano et al., 2013). Therefore, soil respiration shows a  
93 parabolic relationship with soil moisture content with reduced soil respiration rates  
94 under both low and high soil moisture levels (Moyano et al., 2013; Linn & Doran, 1984).  
95 Water table depth regulates soil moisture and oxygen availability, therefore indirectly  
96 determining CO<sub>2</sub> emissions (Evans et al., 2021; Tiemeyer et al., 2020). Carbon availability  
97 is the result of past hydrological conditions, the dominant peat-forming plant species,  
98 plant production, and climate (Loisel et al., 2014). This results in spatial variation in soil  
99 carbon density (i.e. quantity of carbon per peat volume), which in turn contributes to  
100 spatial variation in soil CO<sub>2</sub> emissions. This interdependency means it can be useful to  
101 integrate water table depth and carbon availability into a single predictor variable,  
102 exposed carbon (amount of carbon above groundwater table), which indirectly  
103 determines CO<sub>2</sub> emissions (Aben et al., 2024). In addition to these, seasonal variation in  
104 temperature and water table depth also determine soil CO<sub>2</sub> emissions (Armstrong et al.,  
105 2015). Consequently, combining multiple drivers of field-scale emissions is necessary  
106 for accurate modelling of the effects of management measures and spatiotemporal  
107 variation in peatland soil CO<sub>2</sub> emissions, as changes in management will affect these  
108 field-scale drivers.

109 In the Netherlands, peat soils are responsible for an estimated  $\pm 25$  % of the GHG  
110 emissions of the agricultural sector, underlining the need for management measures to  
111 reduce these emissions (Baren et al., 2024). An often proposed management measure is  
112 the combination of topsoil removal (TSR) with rewetting (groundwater table rise) or



113 paludiculture (wet agriculture) where TSR, the removal of the topsoil varying between 5  
114 cm and 60 cm in depth, is effective in removing labile carbon and nutrients that have  
115 typically accumulated as a consequence of long-term drainage (Zak et al., 2010; Brouns  
116 et al., 2014). This removal reduces CH<sub>4</sub> emissions that usually follow a rise in  
117 groundwater table and eutrophication of surrounding surface water (Harpenslager et al.,  
118 2015; Zak et al., 2017; Huth et al., 2020; Quadra et al., 2023; Käärmelahti et al., 2024; Van  
119 Den Berg et al., 2024). Although TSR and rewetting have been proposed as measures for  
120 reducing GHG emissions from peatland meadows, their implementation at large scales  
121 is currently not feasible in areas used for agricultural production due to the loss of  
122 productivity, and resulting economic and political consequences. Nevertheless, in Dutch  
123 peatland meadow areas TSR is currently used as part of a set of management practices  
124 designed to enhance the biodiversity in the border zones of field border ditches and to  
125 improve water quality by increasing nutrient retention in these ditch borders. These  
126 practices, also referred to as regenerative ditch borders (or nature-friendly ditch  
127 margins), are actively stimulated by Dutch waterboards (regional governing bodies  
128 responsible for water management) (van Vossen & Verhagen, 2009). Regenerative ditch  
129 borders also have great potential to contribute to CO<sub>2</sub> emission reductions which is  
130 currently overlooked. This is important, as a negative side effect of TSR occurs when the  
131 removed soil mineralizes and releases CO<sub>2</sub> when placed under aerobic conditions (Van  
132 Den Berg et al., 2024). The resulting accrued carbon debt needs to be accounted for, as  
133 it can substantially delay net carbon emission reductions and the realization of climate  
134 benefits (Huth et al., 2022; Van Den Berg et al., 2024). It is therefore important to estimate  
135 the effectiveness of TSR in reducing CO<sub>2</sub> emissions, as TSR is a widely proposed and  
136 implemented management measure with possible carbon trade-offs.

137 Implementing TSR in ditch borders will cause changes in local abiotic conditions in the  
138 peat soil, as excavation creates a gradual slope that extends from five meters into the  
139 field and descends to the point where the water's edge is met. The newly created topsoil  
140 is therefore positioned closer to the water table (i.e. lower elevation level) than topsoil  
141 pre-TSR leading to increased frequency of water saturated conditions in these upper soil  
142 layers. Especially during the dry summer periods, when groundwater levels are lower, the  
143 surface layers of soils in these ditch borders remain wetter in comparison to soils in



144 conventional ditch borders. As temperature effects are more profound when peat soils  
145 are drier (Kechavarzi et al., 2010), wetter conditions during summer can therefore  
146 potentially buffer temperature effects on soil respiration (Fernández-Pascual & Correia-  
147 Álvarez, 2021). In addition to these changes in soil temperature and moisture conditions,  
148 excavation also directly reduces the total amount of carbon exposed to oxygen under a  
149 given surface area. All these effects of TSR are co-occurring and influenced by  
150 seasonality, such that the mechanisms expected to lead to CO<sub>2</sub> emission reduction are  
151 intertwined. It's therefore challenging to attribute the effectiveness of regenerative ditch  
152 borders to a single parameter (Armstrong et al., 2015). This is of particular importance,  
153 given that parameter effects may change in magnitude over the seasons and with respect  
154 to one another. While parameters can explain variation in soil respiration independently  
155 of seasonality, the extent to which other parameters can explain variation may change  
156 over time. Understanding of how these parameters change and affect CO<sub>2</sub> emissions will  
157 enhance our ability to predict the emission mitigation potential of regenerative ditch  
158 borders and a range of other potential management measures that aim to reduce CO<sub>2</sub>  
159 emissions from drained peatlands.

160 In this study we aimed to understand how ditch border management affects soil  
161 temperature, soil moisture content, exposed carbon densities and consequently how  
162 this practice influences CO<sub>2</sub> emissions from soil respiration in lowland managed peat  
163 meadows in the Netherlands. We established a year-round field survey in which we  
164 measured soil respiration in conventional vs. topsoil-removed regenerative ditch  
165 borders. Measurements were performed along a transect from the water's edge into the  
166 agricultural field, covering a representative range of soil conditions. Following the field  
167 study, we fit statistical models to assess the effects of soil temperature, moisture, and  
168 carbon densities exposed to oxygen on soil respiration under both ditch border  
169 management types. We then used the best fitting model to answer the following  
170 questions: (1) how do soil temperature, soil moisture content and exposed carbon relate  
171 to spatiotemporal variation in soil respiration?; (2) what is the effect of regenerative ditch  
172 borders (i.e. TSR) on seasonal and annual modelled soil respiration?; (3) to what extent  
173 do soil temperature, soil moisture content, and exposed carbon contribute to differences  
174 in soil respiration between conventional and regenerative ditch borders throughout the



175 measuring period?; and (4) over what timescale do eventual changes in soil respiration  
176 rates compensate for possible carbon debts resulting from TSR?

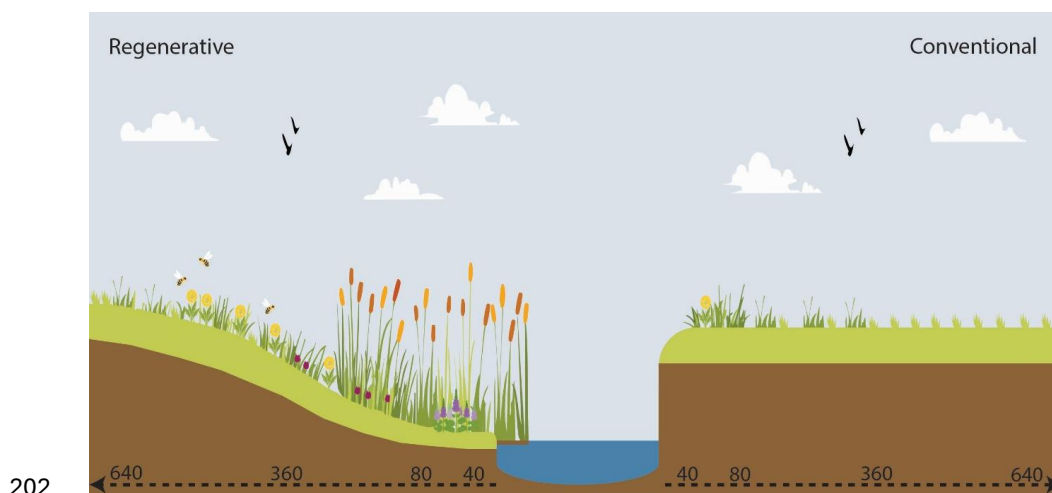
177

## 178 2 Material & Methods

### 179 2.1 Study area

180 The study area was located in the Vereenigde Binnenvolde, Spaarnwoude, province of  
181 North Holland, the Netherlands (52°40'34.1" N, 5°9'55.4" E). This minerotrophic peat  
182 polder has been described in detail in previous research (Bethe et al., 2025). The  
183 dominant land-use of the polder is conventional livestock farming and consists of  
184 grasslands separated by ditches. In 1997, a total of 4 ha of multiple regenerative ditch  
185 borders (RDB) were constructed by excavating the topsoil layer creating a gentle down-  
186 hill slope starting from five meters into the agricultural field and continuing towards the  
187 waterside (Fig. 1). After the RDBs were established, management in these borders was  
188 adjusted to no manure use, no or delayed mowing, and no biomass harvesting. In the  
189 same polder, the remaining ditch borders (hereafter conventional ditch borders - CDB)  
190 were subjected to the same management as the adjoining agricultural field apart from a  
191 mandatory 1.5 m buffer zone (measured from the water's edge) where no manure use  
192 was allowed. This zone was still subject to regular mowing (1-3 times a year) for hay  
193 production (Rijksdienst voor Ondernemend Nederland, 2024). In both RDBs and CDBs  
194 the agricultural fields were subject to cattle grazing with comparable cattle stocking  
195 densities. In RDBs, TSR resulted in substantial vegetational changes (Fig. 1). Close to the  
196 water's edge, the vegetation was dominated by *Phragmites australis* with *Mentha*  
197 *aquatica* patches in between and further up the slope a variety of herb and grass species,  
198 such as *Lolium perenne* and *Lotus pedunculatus*. In CDBs, the vegetation was  
199 dominated by grass species, such as *Lolium perenne*, with some herb species, such as  
200 *Ranunculus repens*, growing closer to the water's edge.

201



202

203 Fig. 1: Schematic comparison between the two ditch border types investigated in this  
204 study; a conventional ditch border (right; CDB) and a regenerative ditch border (left; RDB)  
205 with a ditch in the middle (blue). In the RDB, a down-hill slope was established by topsoil  
206 removal (TSR) from the field towards the water's edge. Distances to the water's edge (see  
207 experimental design) 40 cm, 80 cm and 360 cm from the water's edge were therefore  
208 located at a lower elevation than corresponding distances in CDBs. Distance 640 cm was  
209 located outside the excavation range in RDBs. A buffer zone was located in the CDBs  
210 extending 1.5 m into the field from the water's edge. In RDBs, TSR coincided with  
211 vegetational changes. Close to the water's edge *Phragmites australis* dominated, while  
212 further along the slope herbs and grasses coexisted. In CDBs, the vegetation mostly  
213 consisted of grasses (e.g. *Lolium perenne*) with some herbs.

214

## 215 2.2 Experimental design

216 Throughout the polder, we selected 20 ditch borders (DBs) of which in 16 DBs the topsoil  
217 was removed to create a RDB and four DBs which were left intact (CDB). We included  
218 more regenerative borders to account for the variation in slopes and management after  
219 excavation. In each of the selected DBs we established four sampling points along a  
220 linear transect starting at the water's edge and going perpendicular to the ditch into the  
221 agricultural field, at 40 cm, 80 cm, 360 cm and 640 cm from the water's edge. Given that  
222 the RDBs were typically five meters wide, at these ditches, the distances 40 cm, 80 cm



223 and 360 cm were located in the excavated area and distance 640 cm was located in the  
224 agricultural field.

225 In all DBs a permanent datalogger (TOMST, TMS-4) was installed at distance 360 cm to  
226 record soil moisture content (at a depth of -14 cm; Time-Domain transmission method  
227 using 2.5 GHz electromagnetic pulses) and soil and air temperature (at soil depth of -6  
228 cm, and +2 cm and +15 cm above the soil surface; MAXIM/DALLAS/ semiconductor  
229 DS7505U+ sensors), measured every 15 minutes (Wild et al., 2019). The dataloggers were  
230 protected from disturbance by livestock with stainless steel bars and were running  
231 throughout the experiment. Data was extracted using Lolly software (version 1.51). For  
232 every DB, we characterized the height profile of the study area by measuring the height  
233 relative to the ditch water level at 40 cm intervals perpendicular to the ditch (0 cm) to the  
234 fourth distance (640 cm) using a theodolite in April 2023. The height profile was made at  
235 a 1 m distance from the measurement transect to minimize disturbance. We also  
236 measured the height at each transect point relative to the ditch water level once.

237

### 238 2.3 Soil respiration measurements

239 Soil respiration ( $R_{soil}$ ) was measured five times throughout the period between June 2023  
240 and March 2024 (June-August-October-January-February/March) at each distance at the  
241 water's edge across all DBs. Additionally, we measured soil respiration more frequently  
242 at a subset of the DBs (2 CDBs and 4 RDBs in July-September-December) to ensure we  
243 captured adequate seasonal variation in soil respiration.  $CO_2$  was measured using a  
244 canopy assimilation chamber (145 mm × ø 146 mm) connected to an infrared gas  
245 analyzer (IRGA; EGM-5 Portable  $CO_2$  Gas Analyzer, PP Systems), equipped with a soil  
246 moisture (mV) and temperature probe (°C) measuring at a soil depth between 0 and -5  
247 cm (Stevens HydraProbe). The chamber was equipped with a PAR sensor and a  
248 temperature sensor (Precision Thermistor). A plastic skirt was attached to the chamber  
249 over which a steel chain was placed to prevent air leakage during measurements. The  
250 chamber was covered with a light-blocking cover. Prior to the measurements, all the  
251 above-ground vegetation in the measurement area was clipped. To avoid excessive  
252 compression/disturbance of the soil close to the chamber, a ladder was placed on the



253 adjacent soil from which the measurements were executed. The chamber CO<sub>2</sub>  
254 concentration (in ppm), soil moisture content, soil and air temperature, and PAR were  
255 measured every second over a period of two minutes of which the first 12 seconds were  
256 discarded.

257 The CO<sub>2</sub> flux rate ( $F_{rate}$ ) for each sampling moment was then calculated (see eq. 1) (Möhl  
258 et al., 2023):

259

$$260 \quad F_{rate} = \frac{\Delta CO_2 \times P \times 273.15}{22.4 \times (273.15 + T_{air}) \times P_i} \times \frac{V}{A} \times 1000 \quad (\mu mol \ CO_2 \ m^{-2} \ s^{-1})$$

261

(eq. 1)

262 Where  $\Delta CO_2$  is the estimated slope from a linear regression of CO<sub>2</sub> over time ( $\Delta[CO_2]/\Delta t$ ),  
263 P the average air pressure during the measurement (kPa), 273.15 (K) the standard  
264 temperature, 22.4 (L mol<sup>-1</sup>) the molar volume of CO<sub>2</sub>,  $T_{air}$  the air temperature in the  
265 chamber (measured by the Precision Thermistor),  $P_i$  the average air pressure at sea level  
266 (101.325 kPa), V the volume (0.002427 m<sup>3</sup>) of the chamber and A the area of the chamber  
267 cross section (0.0167 m<sup>2</sup>).

268 The calculated  $F_{rate}$  was then converted to CO<sub>2</sub> (g) per m<sup>2</sup> per h using the molar mass of  
269 CO<sub>2</sub> (44.01 g mol<sup>-1</sup>). Throughout the year, some air temperature measurements failed. To  
270 calculate the CO<sub>2</sub> flux in these cases, we performed a linear regression with air  
271 temperature measurements from the HydraProbe and from the permanent datalogger  
272 (+15 cm) to estimate the missing values for air temperature. We calibrated the  
273 HydraProbe, by taking a soil sample (14 cm × ø 18.5 cm) which was cut out of the soil  
274 from one of the sites, watering it back to water holding capacity and then oven drying  
275 (30°C) the sample for a period of two weeks. Soil moisture values from the HydraProbe  
276 were recalculated based on the linear relationship between the HydraProbe values and  
277 gravimetric soil moisture content measured during this drying period.

278 We computed an annual dataset with soil temperature and soil moisture data collected  
279 with the IRGA during CO<sub>2</sub> flux measurements (5 or 8 measuring points). To enable an  
280 annual (one full year) interpolation between the measuring points we duplicated our  
281 dataset and incremented the year in the duplicated set, while leaving all other values



282 unchanged. We then interpolated daily values for soil temperature and moisture by  
283 applying a smoother (span = 0.75) for the period between October 2023 – October 2024  
284 (Fig. S7 and S8 in the Supplement).

285

## 286 2.4 Peat descriptions and soil core profiles

287 Morphological and structural descriptions were made of the peat soil at all DBs at a  
288 distance of 360 cm from the water's edge. We used a gouge auger (Eijkelkamp 04.02.SA;  
289  $\varnothing$  3 cm) to drill to the Pleistocene deposits (100 – 365 cm deep). All visibly distinct peat  
290 layers were identified and described following the description method by Deltares  
291 (Erkens et al., 2013).

292 We collected soil cores (100 cm  $\times$   $\varnothing$  6 cm) at all DBs at a distance of 360 cm from the  
293 water's edge using a gouge auger (Eijkelkamp 04.02.SA). After sampling, we carefully  
294 sliced the cores out of the gouge using a steel wire and wrapped them in foil. The cores  
295 were then placed in PVC tubes and were wrapped in tubular plastic foil to prevent  
296 oxidation by air exposure. The cores were processed in the laboratory within 24 h after  
297 sampling. We took subsamples of the core at 5 cm depth intervals using a cutter (1 cm  $\times$   
298 1 cm  $\times$  5 cm) to determine gravimetric moisture content (SMC) ( $\frac{SMC_{wet} - SMC_{dry}}{SMC_{wet}} * 100\%$ ;  
299 after drying at 70°C for 48 h), bulk density ( $\frac{Dry\ weight}{volume}$ ) and organic matter content through  
300 loss on ignition (550°C for 4 h, muffle furnace). We determined total carbon (C) and  
301 nitrogen (N) content through flash combustion using an elemental analyzer after grinding  
302 the dried soil (FLASH EA 1112). For each of the 20 cores, carbon densities (kg C m<sup>-2</sup>; Fig.  
303 S1 in the Supplement) were calculated for every 5 cm depth interval to 100 cm depth  
304 using the measured total C and bulk density values.

305

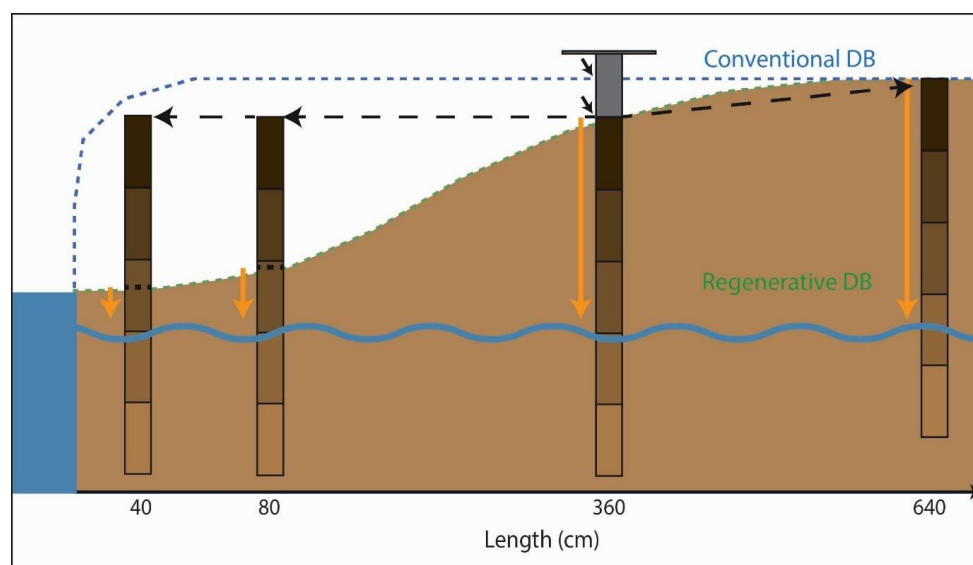
## 306 2.5 Groundwater levels and exposed carbon calculation

307 Groundwater levels were measured 11 times throughout the measuring period at a fixed  
308 site in the polder at 3 m distance from the ditch with a known height relative to the ditch  
309 water level. Groundwater levels were measured in four monitoring wells with different  
310 filter depths (at -25 cm, -50 cm, -100 cm and -150 cm). Due to high hydraulic head and



311 semi enclosed aquifer, the groundwater level was above the phreatic groundwater level  
312 in monitoring wells -100 cm and -150 cm and therefore the groundwater levels measured  
313 in these wells were not used. We used the groundwater data from monitoring well -50 cm  
314 for our calculations. To generate a daily time series of estimated groundwater level for  
315 subsequent modelling, we applied a smoother (span = 0.4) to the data and extracted the  
316 resulting interpolated daily groundwater level values. As the groundwater level was  
317 measured at one site in the polder, we recalculated groundwater levels for all distances  
318 to the water's edge in all DBs by performing a correction based on the relative height to  
319 the ditch water level at the monitoring well to the relative height of all the distances to the  
320 water's edge. We used these distance-specific interpolated daily ground water levels to  
321 calculate daily exposed carbon which was defined as the sum of carbon densities in the  
322 depth intervals above the interpolated groundwater level ( $\text{kg C m}^{-2}$ ) (Fig. 2A, Fig. S9 and  
323 S10 in the Supplement).

324



325

326 *Fig. 2: Schematic representation of the exposed carbon calculation. We sampled 1 m*  
327 *cores at distance 360 cm at all DBs (2 black arrows). In regard to the conventional DBs*  
328 *(blue dashed line; CDB), we assumed that carbon content profiles were equal at all*  
329 *distances to the water's edge and extrapolated the carbon densities at distance 360 cm*



330 to all other distances to the water's edge. For the regenerative DBs (green dashed line;  
331 RDB), we also extrapolated the carbon densities at distance 360 cm to all other distances  
332 to the water's edges (black dashed lines) and for distances 40 cm and 80 cm we  
333 additionally corrected the carbon density profiles for TSR. TSR correction was performed  
334 based on their height differences and the start of the carbon density profile was adjusted  
335 based on this difference. Then exposed carbon values (orange arrows) were calculated  
336 based on the amount of carbon above the groundwater level (blue wavy line).

337

## 338 2.6 Soil respiration modelling

339 To assess how soil temperature, soil moisture content and exposed carbon relate to  
340 spatiotemporal variation in soil respiration and to extrapolate our periodic field  
341 measurements to a full year of soil respiration under a variety of conditions we fit a series  
342 of statistical models to the respiration data. We compared model performance across  
343 four different parameterizations. Soil respiration ( $R_{soil}$ ,  $F_{rate}$  ( $g\ CO_2\ m^{-2}\ h^{-1}$ )), was modelled  
344 as the product of functions of temperature (T), moisture content (M) and exposed carbon  
345 (CE) (see eq. 2).

$$346 \quad R_{soil} = R_{soil-T} * R_{soil-M} * R_{soil-CE}$$

347 (eq. 2)

348 For the  $R_{soil-T}$  and  $R_{soil-M}$  functions we chose model parameterizations that were identified  
349 as effective in previous soil respiration modelling studies (Suseela et al., 2012;  
350 Kechavarzi et al., 2010; Mäkiranta et al., 2009). Specifically, we assumed an exponential  
351 relationship between soil respiration and temperature.

$$352 \quad R_{soil-T} = a e^{(bT)}$$

353 (eq. 3)

354 Where  $R_{soil-T}$  is as defined in equation 2, a (>0) and b (0-1) parameters, and T the observed  
355 soil temperature (°C; soil depth up to -5 cm).

356 We assumed a parabolic relationship between soil respiration and soil moisture content.  
357 The moisture function we used requires fixed minimum and maximum values of soil



358 moisture based on the data. We set the min and max to 10 and 100 % soil moisture  
359 content, respectively, to derive a parabolic function that predicted non-negative soil  
360 respiration over the full range of interpolated soil moisture data in our time series.

361

$$362 \quad R_{soil-M} = (SMC - min)(max - SMC)^c$$

363

(eq. 4)

364 Where  $R_{soil-M}$  is as defined in equation 2, SMC the observed soil moisture content (%), min  
365 a fixed minimum SMC (10), max a fixed maximum SMC (100) and  $c (>0)$  a parameter to be  
366 fit.

367 We tested models with three possible relations between soil respiration and exposed  
368 carbon describing a linear relationship with a fixed intercept at 0 (when  $C_{exp} = 0$   
369  $= R_{soil-CE}$ ), a linear relationship with a free intercept (when  $C_{exp} = 0$ ,  $R_{soil-CE} = h$ ) and a  
370 sigmoidal relationship (see eq. 5, 6 and 7).

$$371 \quad R_{soil-CE} = C_{exp}$$

$$372 \quad R_{soil-CE} = h + iC_{exp}$$

$$373 \quad R_{soil-CE} = \frac{l}{1 + e^{(-n C_{exp})}}$$

374

(eq. 5, 6, and 7)

375 Where  $R_{soil-CE}$  is as defined in equation 2,  $C_{exp}$  the computed amount of carbon above the  
376 groundwater level on the day of the  $F_{rate}$  measurement ( $\text{kg C m}^{-2}$ ),  $h (>0)$ ,  $i (>0)$ ,  $l (>0)$ , and  
377  $n (>0)$  parameters.

378 We tested one soil respiration model with  $R_{soil-T}$  and  $R_{soil-M}$  only and three models  
379 additionally including one of the three  $R_{soil-CE}$  sub-models which led to four fitted soil  
380 respiration models:

$$381 \quad R_{soil} = (a e^{(bT)})((SMC - min)(max - SMC)^c)$$

$$382 \quad R_{soil} = (d e^{(fT)}) * ((SMC - min)(max - SMC)^g) * C_{exp}$$

$$383 \quad R_{soil} = ((h + iC_{exp}) e^{(jT)}) * ((SMC - min)(max - SMC)^k)$$



384 
$$R_{soil} = \left( \frac{l}{1 + e^{(-n \cdot Cexp)}} \right) e^{(mT)} * ((SMC - min)(max - SMC)^o)$$

385 (model 1, 2, 3, and 4, respectively)

386 All four soil respiration models were fit using Bayesian non-linear regression in the ‘brms’  
387 package (Bürkner, 2017). For all models, four Markov chain Monte Carlo (MCMC) chains  
388 were ran with 2000 iterations each and with a 1000 iteration warm-up period. MCMC  
389 chain convergence was evaluated diagnostically through trace plots and density plots.  
390 The four models were compared with Leave-One-Out Cross-Validation (LOO-CV),  
391 comparing the four models by their computed expected log pointwise predictive density  
392 (elpd\_diff) with uncertainty (se\_diff), expressed relative to the top-ranked model (which  
393 has elpd\_diff = 0). We also evaluated the posterior predictive accuracy of the four models  
394 by computing the mean squared error (MSE) by generating posterior-predictive draws and  
395 calculating the mean squared error between the predicted and observed soil respiration  
396 values (mse). Based on these two model evaluation methods, we chose the best  
397 performing model and evaluated the model fit by a residual vs. fitted plot and an observed  
398 vs. predicted plot (Fig. S3 and S4 in the Supplement).

399

## 400 2.7 Carbon debt and payback time: assumptions and calculation

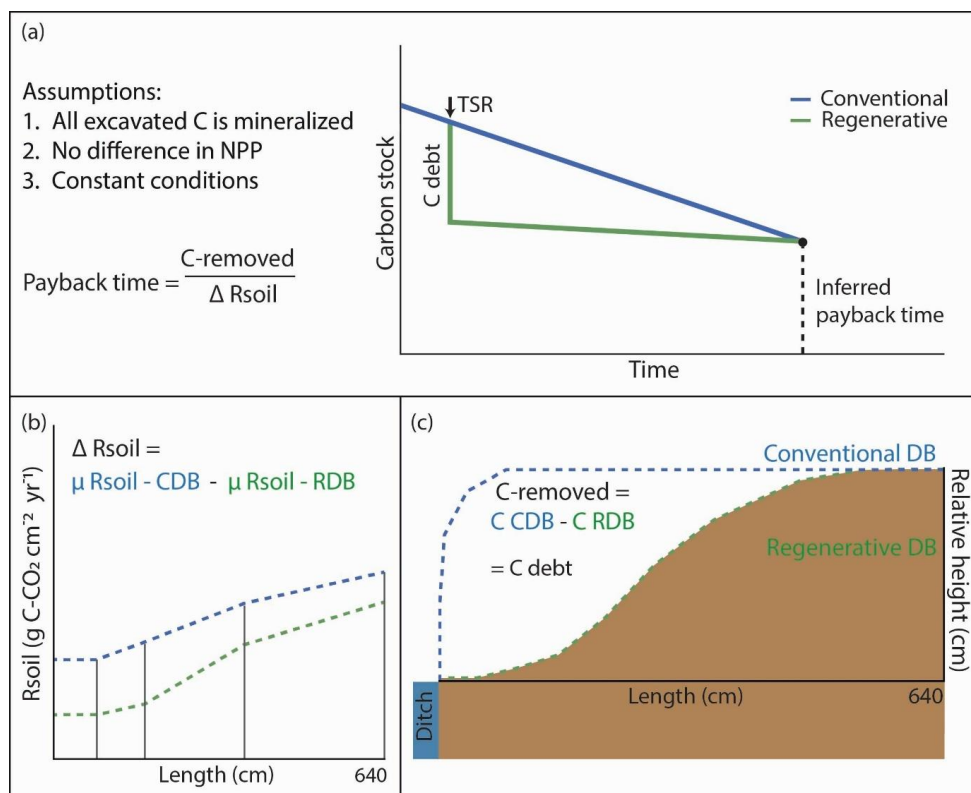
### 401 method

402 We used the model estimates to estimate the ‘payback time’ defined as the number of  
403 years for net negative effects on cumulative CO<sub>2</sub> emissions (net reduced emissions), to  
404 be reached after implementing RDBs. The payback time indicated how many would be  
405 necessary to compensate for soil carbon lost as a result of the intervention. The payback  
406 time was computed by dividing the amount of carbon removed by TSR (C-removed) by  
407 the difference in soil respiration between CDBs and RDBs ( $\Delta R_{soil}$ ). Our approach was  
408 based on three simplifying assumptions: 1) all organic carbon removed during the TSR  
409 procedure was mineralized to CO<sub>2</sub> i.e. the carbon debt was equivalent to the amount of  
410 soil carbon in the removed soil volume; 2) no difference in net primary production  
411 between CDBs and RDBs and, thus, relative changes in carbon stock between border  
412 types were solely driven by differences in soil respiration rates; and 3) the differences in



413 conditions driving  $R_{soil}$  (temperature, moisture content and exposed carbon) remained  
 414 constant over time (Fig. 3a).

415



416

417 Fig. 3: Payback time calculation. (a) The calculation of the inferred payback time was  
 418 based on three assumptions: (1) all excavated carbon (C) was mineralized, (2) no  
 419 difference in net primary production (NPP) between border types and (3) constant  
 420 conditions over time. The assumptions imply that the difference in carbon stock between  
 421 conventional (CDBs; blue) and regenerative ditch borders (RDBs; green) was solely driven  
 422 by their different soil respiration. (b)  $\Delta R_{soil}$  was computed by subtracting the mean ( $\mu$ )  $R_{soil}$ -  
 423  $CDB$  from the  $\mu R_{soil}$ - $RDB$  over the entire length of the transect (0 - 640 cm). C. C-removed  
 424 (carbon debt) was computed by subtracting the mass of carbon above the ditch water  
 425 level RDBs from the corresponding carbon stock of CDBs.

426



427 As our soil respiration measurements only started at 40 cm from the water's edge, we  
428 also had to assume the area in between 0 and 40 cm showed the same respiration rates  
429 and dynamics as the 40 cm measurements and therefore an additional distance of 0 cm  
430 was added to the dataset with data identical to the 40 cm data (Fig. 3b). To determine  $\Delta$   
431  $R_{\text{soil}}$ , annual soil respiration was calculated at every distance to the water's edge ( $\text{g CO}_2$   
432  $\text{cm}^{-2} \text{yr}^{-1}$ ) using the 'trapz' function (R package pracma). Distance to the water's edge was  
433 plotted as an actual distance using a smoother (span = 0.5) between 0-40-80-360-640  
434 cm of which the data was extracted (Fig. 3b). With this data, we calculated the mean  
435 annual soil respiration rate for both DB types by numerical integration using 'trapz'.  $\Delta R_{\text{soil}}$   
436 ( $\text{g C-CO}_2 \text{cm}^{-2} \text{yr}^{-1}$ ) was then computed by subtracting the mean rate of CDBs with the  
437 mean rate of RDBs (Fig. 3b). To determine C-removed, we used 'trapz' to calculate the  
438 total volume of soil under the relative height profiles (volume above water level in ditch  
439 reaching till distance 640 cm into the field) of each DB per meter of ditch border length.  
440 The average of the total volume of all CDBs functioned as a pre-TSR reference of which  
441 the total volume of each RDB was subtracted which was defined as 'removed volume'  
442 ( $\text{cm}^2$ ) (Fig. 3c). We calculated the mean carbon density in three ways: (method 1) a mean  
443 carbon density for each regenerative DB; (method 2) a mean carbon density of the four  
444 conventional borders; and (method 3) a mean carbon density of all the cores combined.  
445 The three mean carbon densities were then multiplied with the 'removed volume' of each  
446 RDB which was defined as C-removed ( $\text{g C cm}^{-2}$ ).

447 Mean payback time was computed by dividing the generated values of C-removed by the  
448 generated values of  $\Delta R_{\text{soil}}$ . We calculated associated uncertainty by performing  
449 parametric bootstrap simulations (Efron & Tibshirani, 1994). We generated a 1000 draws  
450 from normal distributions of C-removed (using the standard error derived from carbon  
451 densities) and of  $\Delta R_{\text{soil}}$  (calculated with three methods using the standard error derived  
452 from difference between the mean rate of conventional borders and regenerative  
453 borders).

454



## 455 2.8 Statistical analysis

456 We extracted the parameter estimates of the best performing model (model 3, see  
457 Results) and used them to calculate daily modelled soil respiration rate values ( $\text{g CO}_2 \text{ m}^{-2} \text{ h}^{-1}$ ) with the interpolated daily temperature, soil moisture content and exposed carbon  
458 values for each distance to the water's edge (example in Fig. S2 in the Supplement).  
459 These daily modelled values were then used to compute estimated annual soil  
460 respiration values for each distance to the water's edge. Due to missing soil temperature  
461 and soil moisture content observations, we excluded distance 40 for DB numbers 1C, 8C  
462 and 12 from further analyses. To analyze the differences in potential drivers across  
463 management types and within DB, we fit separate linear mixed-effects models to the  
464 mean soil temperature, mean soil moisture content, mean exposed carbon, and annual  
465 modelled soil respiration for each distance to the water's edge with DB type (categorical)  
466 and distance to the water's edge (categorical) as fixed effects and DB number as random  
467 effect (Bates et al., 2015). We tested for normality of the residuals using Q-Q plots and  
468 for homogeneity of the variance using residual vs. fitted plots. The models included both  
469 main effects and the two-way interaction and significance of terms was tested using  
470 ANOVA (Kuznetsova et al., 2017). We performed planned contrasts to test for differences  
471 between DB types averaged over each distance to the water's edge and between DB types  
472 within each distance to the water's edge ( $\alpha = 0.05$ ) (Searle et al., 2012). The same  
473 analysis, for annual modelled soil respiration, was repeated without distance 640 cm, as  
474 this distance was located in the agricultural field where differences between DB types  
475 were reasoned to be minimal. Excluding distance 640 cm did not affect the conclusions  
476 of the ANOVA and planned contrast analyses and the distance was kept for analysis.

478 To quantify the relative importance of each of the three predictor variables in contributing  
479 to the model predictions, we computed Shapley Additive Explanations (SHAP) using the  
480 'fastshap' package (Štrumbelj & Kononenko, 2013). For each SHAP evaluation, the  
481 posterior expected value was computed by averaging 200 draws from the posterior  
482 predictive distribution. SHAP values were estimated with Monte Carlo approximation  
483 using 100 simulations per observation, using the full randomized version of the observed  
484 dataset. These values represented each predictor's contribution to the model



485 predictions by averaging its marginal impact across all possible subsets of the remaining  
486 predictors.

487 We performed counterfactual decomposition to determine the relative contributions of  
488 the predictors soil temperature, soil moisture content and exposed carbon in explaining  
489 differences in soil respiration between DB types (Fairlie, 2005). To investigate seasonal  
490 and spatial variation in variable importance, we performed this procedure using model  
491 predictions at all distances to the water's edge and over the entire measuring period. The  
492 predictor values were first averaged over the DB numbers for each DB type × distance to  
493 water's edge × date combination to obtain the daily contributions of the predictors. Soil  
494 respiration predictions were made using model 3 and its parameter estimates (i.e. h, i, j,  
495 and k). Soil respiration at CDBs was used as the reference condition which meant the  
496 values of the predictors soil temperature, soil moisture content and exposed carbon  
497 correspond to soil respiration at CDBs for each distance to the water's edge × date. We  
498 then generated counterfactual predictions in which the value of each predictor, one  
499 predictor at once, was replaced with the corresponding predictor values at RDBs, while  
500 holding the remaining two predictor CDB values. This was repeated for all three  
501 predictors, and over the entire measuring period.

502

## 503 3 Results

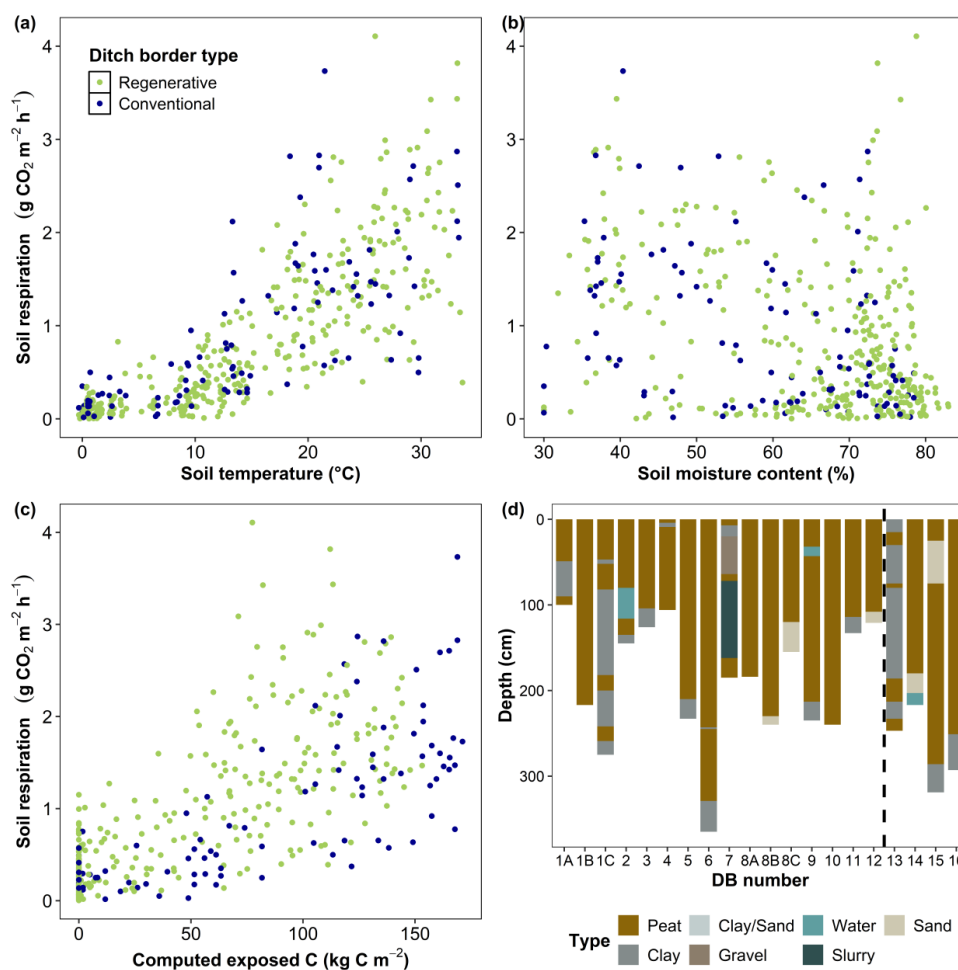
### 504 3.1 Patterns of soil respiration and soil descriptions

505 Soil temperature measurements made during respiration measurement campaigns  
506 displayed seasonal variation from 33.7 °C summer to -0.3 °C in winter, and corresponding  
507 respiration measurements showed an overall positive relationship to soil temperature  
508 (Fig. 4a). The relationship between soil moisture content and soil respiration was less  
509 clear for both DB types (Fig. 4b). Measured soil moisture content ranged from 30 % to 83  
510 %. Overall, soil respiration increased with increasing exposed carbon. Exposed carbon  
511 ranged from 0 kg C m<sup>-2</sup> in winter when groundwater levels were at the soil surface up to  
512 171 kg C m<sup>-2</sup> in summer when groundwater levels were low (Fig. 4c). Peat depth at the 20  
513 DBs varied between 100 cm (DB 1A) and 329 cm (DB 6) (Fig. 4d). There was also



514 considerable variation in the relative distribution and thickness of the different soil layer  
 515 types, in particular DB 13 was rich in clay, which could suggest a previous riverine history,  
 516 and DB 7 had quite a large, disturbed gravel layer in the top 1 m. The botanical origin of  
 517 the majority of the peat was identified as reed (*Phragmites australis*).

518



519

520 Fig. 4: The relationship between measured soil respiration and (a) soil temperature, (b)  
 521 soil moisture content, and (c) computed exposed carbon. Points are colored by DB type  
 522 (regenerative = green (RDB) and conventional = blue (CDB)) and represent the observed  
 523 field data (n = 445). (d) Soil profiles (colors represent different layer types) of all DBs down  
 524 to the mineral layer; the dashed line separates the RDBs (n = 16) from the CDBs (n = 4).



525

526 **3.2 Model fit evaluation & model predictions**

527 The LOO-CV results indicated model 3 to be the best of the candidate models for  
 528 explaining the observed variation in soil respiration (Table 1). The same conclusion was  
 529 drawn based on comparing the MSE, where model 3 had the lowest MSE. Model 3 was  
 530 therefore selected as the best performing model and used for subsequent calculations.

531

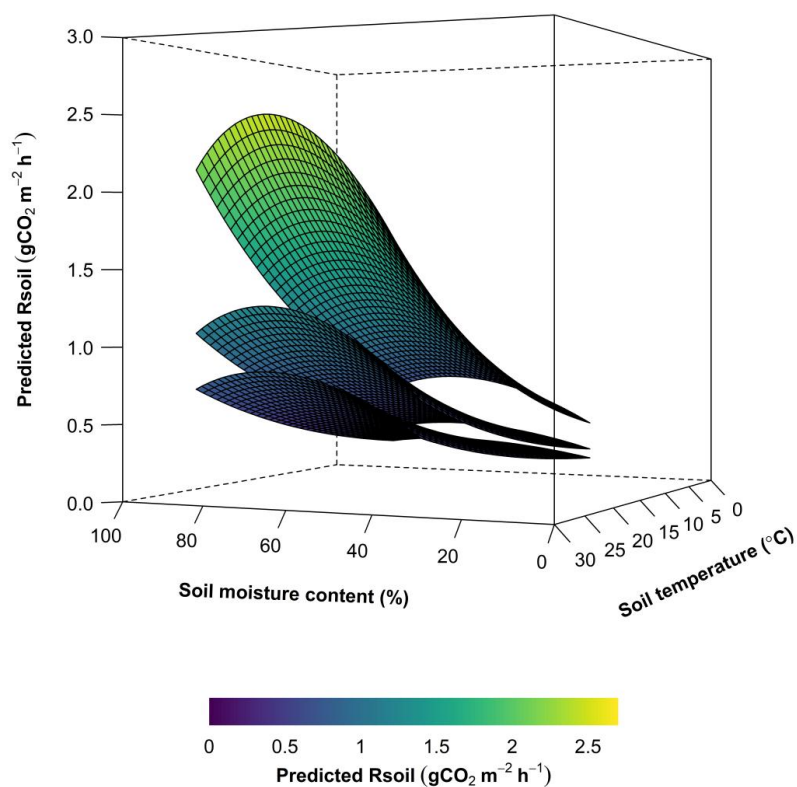
532 *Table 1: Model comparison results of the Leave-One-Out Cross-Validation (LOO-CV) and*  
 533 *Mean Squared Error (MSE) for the four soil respiration models with four possible different*  
 534 *exposed carbon sub-models (see section 4.6). Using LOO-CV, we computed and*  
 535 *compared the log pointwise predictive density with uncertainty (elpd\_diff ± se\_diff) of*  
 536 *each model, expressed relative to the best ranked model (elpd\_diff ± se\_diff = 0). Using*  
 537 *MSE, we compared the posterior predictive accuracy of the models by computing the*  
 538 *mean squared error between the predicted and observed soil respiration values (mse).*  
 539 *The resulting best performing model, resulting from the two model evaluation methods,*  
 540 *is highlighted in bold.*

Models	Exposed C sub-model	Elpd_diff ± se_diff	Mean squared error
1.	-	-28.5 ± 10.2	0.543
2.	~ $C_{exp}$	-47 ± 9	0.585
<b>3.</b>	<b>~ <math>h + iC_{exp}</math></b>	<b>0 ± 0</b>	<b>0.472</b>
4.	~ $\frac{l}{1 + e^{(-n C_{exp})}}$	-3.5 ± 6.6	0.48

541

542 Based on the computed SHAP values, the predictor variables exposed carbon and soil  
 543 temperature had the highest contributions to explaining overall variation in soil  
 544 respiration (model 3), explaining 0.321 and 0.303 of the total variance, respectively (Fig.  
 545 S5 in the Supplement). Soil moisture content explained 0.08. of the variance and together  
 546 the three predictor variables explained 0.704 of the total variance (70 %).

547



548

549 *Fig. 5: Predicted soil respiration ( $R_{soil}$ ;  $g\ CO_2\ m^{-2}\ h^{-1}$ ) for soil temperature ( $^{\circ}C$ ), soil moisture*  
550 *content (%) and three levels of exposed carbon ( $kg\ C\ m^{-2}$ ). Soil respiration predictions*  
551 *were generated based on model 3 ( $h = 5.2e-4 \pm 1.2e-4$ ;  $i = 7.7e-6 \pm 2.7e-6$ ;  $j = 4.4e-2 \pm$*   
552  *$0.41e-2$ ; and  $k = 0.6 \pm 0.071$ ) using the observed range of soil temperature and soil*  
553 *moisture content. Separate prediction surfaces were plotted for the 10th, 50th and 90th*  
554 *percentile of exposed carbon (10th = 0; 50th = 34.2; and 90th = 134.3  $kg\ C\ m^{-2}$ ). Positions*  
555 *of the surface relative to the vertical axis and the colour gradient indicative values of*  
556 *predicted soil respiration.*

557



558 Soil respiration increased with increasing amounts of exposed carbon (Fig. 5 & Fig. S6 in  
 559 the Supplement). For example, at the annual mean soil temperature of 17 °C and soil  
 560 moisture content of 56 %, soil respiration increased by 0.367 g CO<sub>2</sub> m<sup>-2</sup> h<sup>-1</sup> when exposed  
 561 carbon increased by 1 SD. Soil respiration rates peaked at a 65 % soil moisture content  
 562 (Fig. 5).

563

### 564 3.3 Importance of soil temperature, soil moisture content and exposed 565 carbon varied over DB type and distance to the water's edge

566 DB type and distance to the water's edge had no significant effect on mean annual soil  
 567 temperatures (Table 2, Fig. S7 in the Supplement). DB type significantly affected the  
 568 mean soil moisture content. RDBs soils were 11 % wetter than the CDBs when averaged  
 569 over the entire measurement period, with RDBs having a mean of 66 ± 0.067 % (SE) and  
 570 CDBs of 59 ± 0.15 % (Table 2, Fig. S8 in the Supplement). Along the distances, 40 cm and  
 571 80 cm were 14 % and 15 % wetter than 360 cm and 22 % and 23 % than 640 cm,  
 572 respectively. DB type significantly affected the amount of exposed carbon at all the  
 573 distances to the water's edge (Table 2, Fig. S9 in the Supplement). RDBs had 40 %, 48 %, 49 %, and 38 %  
 574 lower exposed carbon than CDBs, respectively from the water into the  
 575 field.

576

577 *Table 2: ANOVA table of the linear mixed-effects model with the observed data*  
 578 *comprising of mean soil temperature, mean soil moisture content, mean computed*  
 579 *exposed carbon, and with modelled predictions comprising of annual modelled soil*  
 580 *respiration as response variable; ditch border type (conventional and regenerative) and*  
 581 *distance to the water's edge (40 cm, 80 cm, 360 cm and 640 cm) as fixed effects; and*  
 582 *ditch border number (1-20) as random effect. The significant p values are highlighted in*  
 583 *bold.*

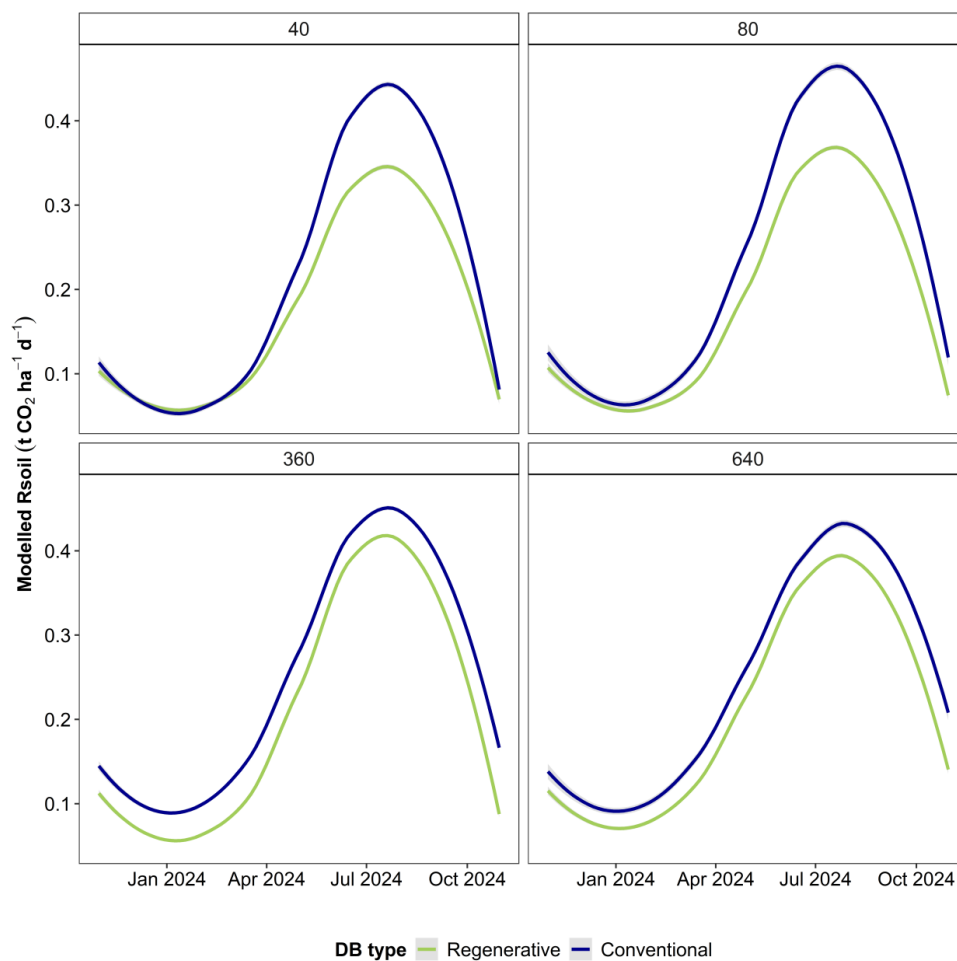
Ditch border type	Distance to the water's edge	Ditch border type × Distance to the water's edge
-------------------	------------------------------	--



		F <sub>1</sub>	p	F <sub>3</sub>	p	F <sub>3</sub>	p
Observed data (n = 80)	Mean soil temperature	0.6	0.467	0.8	0.478	1.4	0.26
	Mean soil moisture content	8.4	<b>0.01</b>	24.5	<b>&lt;0.001</b>	2	0.123
	Mean computed exposed carbon	32.2	<b>&lt;0.001</b>	27.1	<b>&lt;0.001</b>	2.9	<b>0.041</b>
Modelled predictions (n = 77)	Annual modelled soil respiration	9.5	<b>0.006</b>	9.1	<b>&lt;0.001</b>	0.4	0.749

584

585 The computed seasonal patterns in soil temperature, moisture and exposed carbon and  
 586 the model fit together determined the seasonal patterns in predicted soil respiration (Fig.  
 587 6). Along the distances, the mean predicted soil respiration rate was  $0.24 \pm 2e-3$  t CO<sub>2</sub> ha<sup>-1</sup>  
 588 <sup>1</sup> d<sup>-1</sup> in CDBs, exceeding the  $0.20 \pm 0.88e-3$  t CO<sub>2</sub> ha<sup>-1</sup> d<sup>-1</sup> predicted in RDBs. During spring  
 589 and summer, the difference in soil respiration between CDBs and RDBs was most  
 590 apparent at distances 40 and 80 cm (Fig. 6). Where at 40 and 80 cm RDBs emitted on  
 591 average  $0.28 \pm 2.2e-3$  and  $0.29 \pm 2.2e-3$  t CO<sub>2</sub> ha<sup>-1</sup> d<sup>-1</sup> and CDBs  $0.35 \pm 4.6e-3$  and  $0.37 \pm$   
 592  $4.8e-3$  t CO<sub>2</sub> ha<sup>-1</sup> d<sup>-1</sup>, while at 360 and 640 cm RDBs emitted on average  $0.33 \pm 2.1e-3$  and  
 593  $0.33 \pm 2e-3$  t CO<sub>2</sub> ha<sup>-1</sup> d<sup>-1</sup> and CDBs  $0.37 \pm 3.5e-3$  and  $0.36 \pm 3.8e-3$  t CO<sub>2</sub> ha<sup>-1</sup> d<sup>-1</sup>  
 594 (respectively).



595

596 *Fig. 6: Modelled soil respiration ( $R_{soil}$ ;  $t\ CO_2\ ha^{-1}\ d^{-1}$ ) over a one-year period showing the*  
597 *mean effect of regenerative (green; RDB) and conventional (blue; CDB) DBs at the four*  
598 *distances to the water's edge (40 cm, 80 cm, 360 cm and 640 cm). Model predictions*  
599 *were computed from the annual interpolated datasets of soil temperature, soil moisture*  
600 *content, and exposed carbon using the model parameter estimates from model 3. The*  
601 *fitted lines represent the overall modelled soil respiration for each DB type (loess*  
602 *smoothed conditional means, span = 0.75).*

603

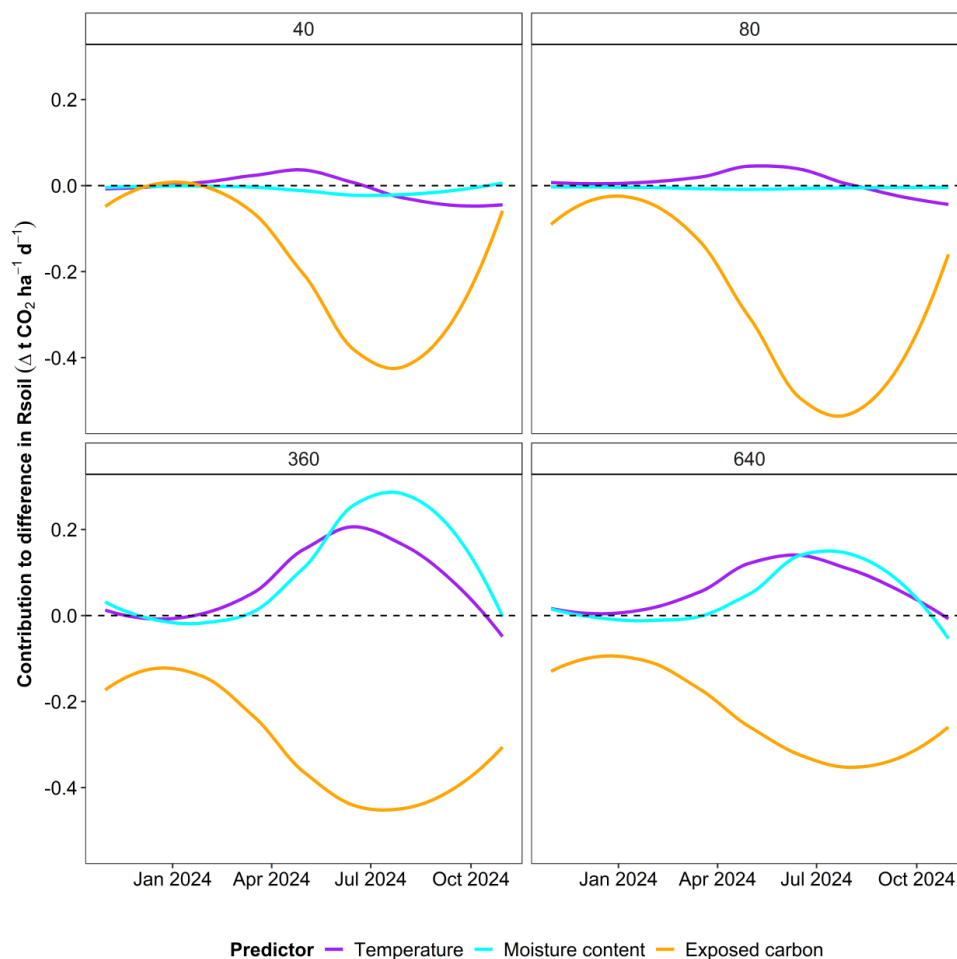
604 The relative importance of the three different predictor variables in explaining variation  
605 between DB types depended on the distance to the water's edge. At distance 40 and 80



606 cm, there was almost no difference in soil respiration between CDBs and RDBs (Fig. 7).  
607 During spring and summer the difference between DB types was more profound (Fig. 6)  
608 which was driven by differences in exposed carbon (Fig. 7). Lower amounts of exposed  
609 carbon in RDBs resulted in lower respiration rates in the spring and summer period (Fig.  
610 6, Fig. S9 in the Supplement). The contributions of variation in soil temperature and soil  
611 moisture content remained near zero throughout the entire measuring season at these  
612 distances. In contrast, at distances 360 and 640 cm, predicted soil respiration was  
613 slightly lower in RDBs throughout the entire measuring season due to lower amounts of  
614 exposed carbon and this effect was more pronounced during spring and summer (Fig. 7).  
615 Also for these distances, lower amounts of exposed carbon in RDBs resulted in lower  
616 respiration rates throughout the year and most strongly in spring and summer (Fig. 6 &  
617 Fig. 7, and Fig. S9 in the Supplement). The contributions of variation in soil temperature  
618 and soil moisture content were minimal during winter, however became more  
619 pronounced during spring and summer (Fig. 7). Higher temperatures and soil moisture  
620 content during this period resulted in higher respiration rates in RDBs (Fig. 6, Fig. S7 and  
621 S8 in the Supplement). The opposing contributions of exposed carbon on the one hand  
622 and soil temperature and moisture content on the other hand therefore diminished any  
623 substantial differences between the DB types at 360 and 640 cm. However, averaged over  
624 the whole year and across the four distances to the water's edge, the overall higher  
625 contribution of exposed carbon resulted in lower soil respiration in RDBs throughout the  
626 year (Fig. 7).

627

628



629

630 *Fig. 7: Contributions of variation in the predictors soil temperature (purple), soil moisture*  
 631 *content (blue) and exposed carbon (orange) to differences in modelled soil respiration (Δ*  
 632 *g CO<sub>2</sub> ha<sup>-1</sup> d<sup>-1</sup>) between conventional (CDB) and regenerative (RDB) DBs for the four*  
 633 *distances to the water's edge (40 cm, 80 cm, 360 cm and 640 cm). The contributions were*  
 634 *computed with counterfactual decomposition. Lines represent the mean daily*  
 635 *contribution of each predictor to the difference between CDBs and RDBs with CDB as the*  
 636 *reference. Positive values indicate that the difference in the predictor variable between*  
 637 *the DB types at the corresponding time point leads to higher predicted respiration rates*  
 638 *and negative values indicate that the difference in the predictor variable between the DB*  
 639 *types at the corresponding time point leads to lower predicted respiration rates in*



640 *regenerative DBs. A value of 0 indicates that there is no difference in the predictor variable*  
641 *between the DB types and therefore does not contribute to a difference in predicted*  
642 *respiration rates. The sum of the daily contributions of soil temperature, soil moisture*  
643 *content, and exposed carbon is equal to the total difference in mean modelled soil*  
644 *respiration between CDBs and RDBs at the corresponding time point (visible in Fig. 6).*

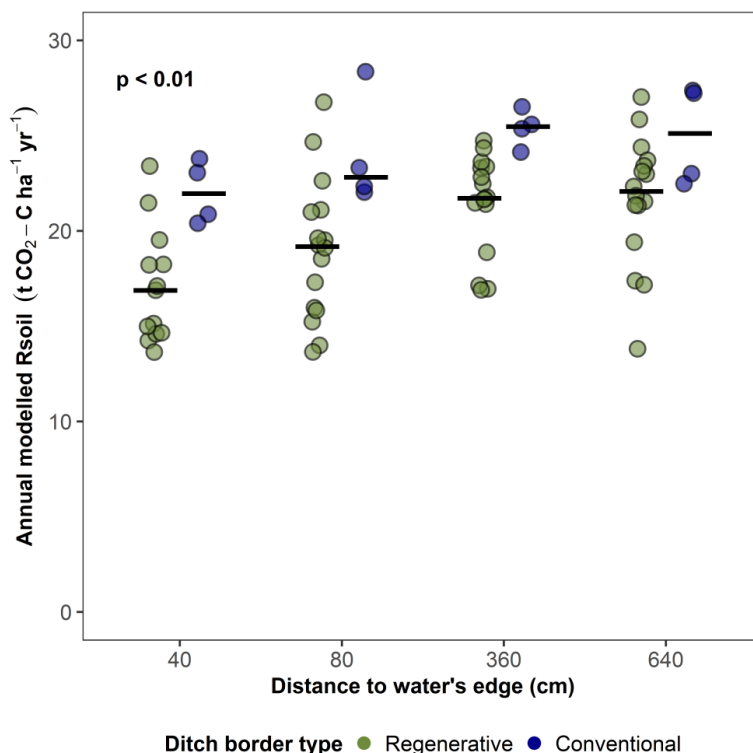
645

### 646 3.4 Regenerative ditch borders had lower predicted soil CO<sub>2</sub> emissions

647 Modelled total annual soil respiration differed significantly between DB types (Table 2).  
648 Averaged across the four distances, RDBs emitted an estimated  $19.9 \pm 0.46$  t CO<sub>2</sub>-C ha<sup>-1</sup>  
649 yr<sup>-1</sup> and CDBs  $24.1 \pm 0.6$  t CO<sub>2</sub>-C ha<sup>-1</sup> yr<sup>-1</sup>, a reduction of 17 % (Fig. 8). Distance to the  
650 water's edge also affected the annual modelled soil respiration (Table 2), where distance  
651 40 cm emitted  $18 \pm 0.84$  t CO<sub>2</sub>-C ha<sup>-1</sup> yr<sup>-1</sup> which was 18 % less than the  $22.2 \pm 0.64$  and  
652  $22.3 \pm 0.78$  t CO<sub>2</sub>-C ha<sup>-1</sup> yr<sup>-1</sup> emitted at distances 360 and 640 cm, respectively.

653

654



655

656 *Fig. 8: Annual modelled soil respiration ( $R_{soil}$ ;  $t\ CO_2-C\ ha^{-1}\ yr^{-1}$ ) for the four distances to the*  
 657 *water's edge (40 cm, 80 cm, 360 cm and 640 cm) in conventional (blue; CDB) and*  
 658 *regenerative (green; RDB) DBs. Each point (jittered) was derived from predictions made*  
 659 *based on the interpolated annual datasets of soil temperature, soil moisture content and*  
 660 *exposed carbon using model estimates (model 3) for each DB × distance to the water's*  
 661 *edge combination. Each black bar shows the mean annual modelled soil respiration for*  
 662 *each DB type × distance to the water's edge combination. P-value represents the overall*  
 663 *effect of DB type, computed from a linear mixed-effects model.*

664

### 665 3.5 Carbon debt increased time before net reductions in CO<sub>2</sub> 666 emissions can be reached

667 The estimated removed carbon due to TSR (carbon debt) varied depending on which  
 668 method was used to quantify the carbon density and ranged between  $450 \pm 4.2$  (method



669 1) –  $458 \pm 0.6$  (method 2), and  $-490 \pm 1.5$  (method 3) g C cm<sup>-2</sup>. The integrated mean  
670 respiration rate in CDBs was estimated at  $0.248 \pm 2.9e-3$  g C cm<sup>-2</sup> yr<sup>-1</sup> and in RDBs at  $0.207$   
671  $\pm 2.4e-3$  g C cm<sup>-2</sup> yr<sup>-1</sup>. Combining these estimates, resulted in an estimated payback time  
672 of  $109 \pm 39$  (method 1),  $119 \pm 42$  (method 2), or  $111 \pm 40$  (method 3) (parametric bootstrap,  
673 SE) years until RDBs show net reduced CO<sub>2</sub> emissions in comparison to CDBs.

674

## 675 4 Discussion

676 We showed that incorporating exposed carbon into models with soil temperature and soil  
677 moisture content led to improved predictions of soil respiration. Exposed carbon and soil  
678 temperature explained the majority of the variation in soil respiration. Soil respiration  
679 peaked at 65 % soil moisture content and was lower in RDBs in comparison to CDBs over  
680 the whole transect. This difference was greatest during spring and summer. While at  
681 distances 40 and 80 cm reductions in predicted soil respiration were driven by lower  
682 amounts of exposed carbon, at distances 360 and 640 cm raised soil temperatures and  
683 moisture content mostly cancelled out reductions in soil respiration by lower amounts of  
684 exposed carbon. Exposed carbon was the foremost driver in differences between CDBs  
685 and RDBs and soil temperature mostly drove temporal patterns in soil respiration. On an  
686 annual basis, RDBs reduced soil CO<sub>2</sub> emissions by 17 % in comparison to CDBs.  
687 However, additional calculations indicate that this reduction due to RDBs, and the  
688 potential carbon debt incurred if carbon in removed topsoil is fully mineralized, imply that  
689 a period of multiple decades is required before DB management results in a net reduction  
690 in cumulative CO<sub>2</sub> emissions relative to the status quo.

691

### 692 4.1 Soil respiration modelling: exposed carbon and soil temperature 693 drive variation in soil respiration

694 The potential CO<sub>2</sub> production from aerobic peat topsoil in the Netherlands can reach  
695  $19.9 \pm 13.6$  t CO<sub>2</sub>-C ha<sup>-1</sup> yr<sup>-1</sup> (i.e.  $200 \pm 137$  kg CO<sub>2</sub> ha<sup>-1</sup> d<sup>-1</sup>) (Boonman et al., 2025). Our  
696 estimates of annual CO<sub>2</sub> productions are consistent with Boonman et al. (2025) which



697 provides support for the model predictions and estimates reported in this study. Soil  
698 moisture content explained only a small proportion of variation in soil respiration,  
699 however showing consistent patterns with other studies. Our model predicted the  
700 highest soil CO<sub>2</sub> production at a moderate soil moisture content (65 %), which likely  
701 reflects the balance between opposing effects of soil moisture on O<sub>2</sub> availability and  
702 substrate diffusion (Fairbairn et al., 2023; Linn & Doran, 1984). Exposed carbon and soil  
703 temperature both explained a substantial part of the variation in soil respiration. Soil  
704 temperature is known to drive seasonal variation in soil respiration rates (Lloyd & Taylor,  
705 1994; Minkinen et al., 2007; Mäkiranta et al., 2009). The importance of exposed carbon  
706 in our soil respiration model indicated that the amount of material available to aerobic  
707 decomposition processes is also influencing soil respiration rates. A previous analysis of  
708 annual carbon budgets in different peatland sites across the Netherlands found that  
709 higher values of net ecosystem carbon balance (i.e. carbon loss from the soil-vegetation  
710 system) correlate with higher amounts of exposed carbon (Aben et al., 2024). In this study  
711 we showed that exposed carbon also drives temporal variation in soil respiration between  
712 peat meadows within one peat site.

713 Although soil temperature, soil moisture content and exposed carbon are known to be  
714 key drivers, there are other important (biotic) drivers of soil respiration that were not  
715 included in this study and could drive variation in soil respiration unexplained by the  
716 predictors in our model. Root exudates are easily decomposable compounds and can  
717 promote fast decomposition in soils (Kuzyakov, 2010). Vegetation shifts accompanying a  
718 change from CDBs to RDBs (i.e. from a *Lolium perenne* to *Phragmites australis*  
719 dominance) can result in changes in the supply of root exudates. *Lolium perenne* is  
720 known to release high amounts of root exudates into the soil which could have  
721 contributed to higher soil respiration rates at the conventional sites (Kuzyakov et al.,  
722 2001). Consequently, vegetation-induced effects could also possibly explain differences  
723 in soil respiration. This effect would be stronger close to the water's edge where almost  
724 all of *L. perenne* is replaced by *P. australis*. Besides vegetation, microbial communities  
725 can also respond to the induced changes in soil conditions. Changes in soil moisture  
726 conditions, for instance, can alter microbial, mesofaunal and macrofaunal communities



727 and could therefore potentially affect soil respiration rates (Laiho et al., 2001; Mäkiranta  
728 et al., 2009; van Dijk et al., 2009; van der Laan et al., 2025).

729 It is important to note that our soil respiration rates could possibly be an overestimation  
730 of the actual soil respiration rates, due to some sources of disturbance. Firstly, the  
731 vegetation was clipped before every field measurement which is known to potentially  
732 overestimate measured soil respiration rates (Li & Sun, 2011). However, this effect would  
733 be equal for all measurements and is unlikely to affect our conclusions on the effects of  
734 DB management. Interpolation of soil respiration rates will have introduced additional  
735 uncertainty and possibly led to missing or overrating peaks of soil respiration. As the DB  
736 sites in this study were in close proximity to each other, it is likely that they experienced  
737 similar climatic conditions, and similar peaks which reduces the effect of dissimilarity  
738 between sites that were possibly uncaptured in our interpolated data. We therefore  
739 consider the effect of these potential sources of error on the validity of our overall results  
740 to be negligible.

741

#### 742 4.2 Reduced soil respiration in regenerative ditch borders

743 RDBs effectively reduced soil respiration rates throughout the entire ditch border (17 %),  
744 which can be mostly attributed to lower amounts of exposed carbon throughout the year  
745 in comparison to CDBs. During prolonged periods of drainage, increased decomposition,  
746 consolidation and shrinkage coincide and compress and compact the aerated top layer  
747 (Galloway et al., 2016; Leifeld et al., 2011). These processes alter the soil properties and  
748 often result in a higher bulk density and mineral fraction, and a reduced pore volume in  
749 this layer. TSR removes the majority of this degraded amorphous topsoil and exposes a new  
750 less degraded peat layer (Van Den Berg et al., 2024). This is partly visible in our carbon  
751 density profiles, made at distance 360, which was more apparent at distances 40 and 80  
752 cm due to deeper TSR depths here. The newly exposed topsoil layer is also known to  
753 contain lower levels of easily degradable carbon and to reduce the mobilization of  
754 dissolved organic carbon (Daun et al., 2026). This can all contribute to reduced soil CO<sub>2</sub>  
755 emissions (Harpenslager et al., 2015; Huth et al., 2020; Daun et al., 2026). However,  
756 reduced soil CO<sub>2</sub> emissions could be the result of changes in electron acceptor



757 availability. RDBs had higher groundwater levels which control the oxygen availability in  
758 the peat soil and therefore aerobic peat decomposition which is captured in exposed  
759 carbon. It is likely that reduced exposed carbon through reduced oxygen availability is  
760 driving reductions in annual soil CO<sub>2</sub> emissions. Previous research on the effects of water  
761 infiltration systems to reduce peat decomposition also emphasize that the effectiveness  
762 of this measure is tightly linked to reductions in water table depth or exposed carbon  
763 (Aben et al., 2024). When these reductions were insufficient, the effect on the net  
764 ecosystem carbon balance was minimal.

765 So far, most studies have focused on TSR in combination with rewetting through  
766 groundwater management (Harpenslager et al., 2015; Zak et al., 2017; Huth et al., 2020;  
767 Quadra et al., 2023; Käärmelahti et al., 2024; Van Den Berg et al., 2024). In the case of  
768 RDBs, no changes in groundwater management take place after the gradual slope is  
769 constructed by TSR. We showed that RDBs were effective in reducing soil CO<sub>2</sub> emissions,  
770 however there are certain combinations of predictor conditions where RDBs have higher  
771 predicted soil respiration which may warrant some caution in applying this measure. In  
772 the middle of the RDB, the soil moisture content was around the optimum level for soil  
773 respiration in spring and summer (60-65 %). Under conditions where the reductions in  
774 exposed carbon are minimal to counteract the effects of optimal moisture conditions  
775 (e.g. minimal excavation & high groundwater table), elevated soil CO<sub>2</sub> emissions might  
776 occur. A similar effect occurred with subsoil irrigation, where water inputs during dry  
777 summer months raised moisture levels in the upper 40 cm into the range that optimizes  
778 microbial decomposition, thereby increasing CO<sub>2</sub> emissions (Weideveld et al., 2021).  
779 Nevertheless, we showed that TSR implemented when constructing RDBs along ditches  
780 is effective in reducing soil CO<sub>2</sub> emissions along the entire DB length. Our study suggests  
781 that TSR without additional rewetting interventions in the form of RDBs, can therefore be  
782 implemented to reduce CO<sub>2</sub> emissions while also providing biodiversity benefits (Renou-  
783 Wilson et al., 2019).

784 Our study focused solely on soil respiration, a complete carbon budget is necessary to  
785 assess the full impact of this measure. We already know vegetation shifts (Fig. 1) are  
786 occurring as a result of RDB construction (Bethe et al., 2025, shift to *Phragmites australis*  
787 dominance), which could be expected to result in differences in net primary production



788 (NPP). *Phragmites australis* is known for its high biomass and primary productivity (Brix  
789 et al., 2001), and shifts to reed dominance could therefore lead to more biomass  
790 available for decomposition, which could therefore reduce the suppressing effect of  
791 RDBs on soil CO<sub>2</sub> emissions. However, measuring the full CO<sub>2</sub> balance remains difficult  
792 with the presence of *P. australis* due to the need for very large flux chambers. Another  
793 caveat in estimating the effectiveness of RDBs, is information on CH<sub>4</sub> emissions. CH<sub>4</sub>  
794 emissions usually start playing a role under inundated conditions and are usually  
795 minimal in drained peatlands (Hendriks et al., 2007; Huang et al., 2021; Boonman et al.,  
796 2025). Even though RDBs promotes wetter conditions and thus possibly CH<sub>4</sub> emissions,  
797 TSR typically ensures low CH<sub>4</sub> emissions in combination with wetter conditions (Huth et  
798 al., 2020; Käärmelahti et al., 2024; Van Den Berg et al., 2024). *Phragmites australis* growth  
799 can promote CH<sub>4</sub> emissions by enhancing CH<sub>4</sub> transport through aerenchyma or reduce  
800 CH<sub>4</sub> emissions by increased oxygenation of the sediment (Boonman et al., 2023; Minke  
801 et al., 2016). Although the effect of DB management on the net ecosystem carbon  
802 balance would give many insights, measuring it remains labor-intensive and costly.

803

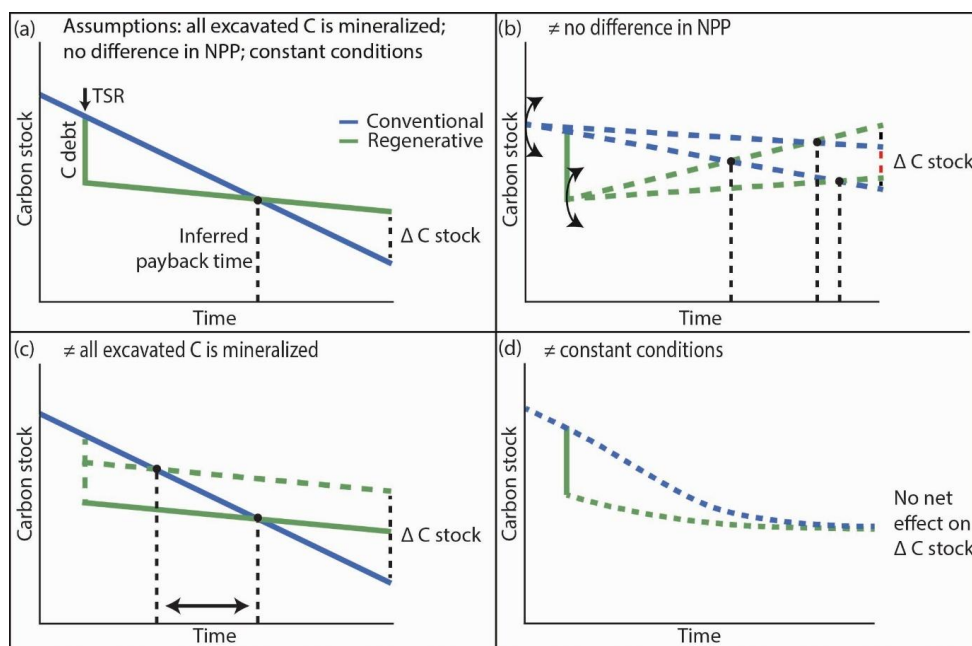
#### 804 4.3 Compensation of soil carbon lost during TSR may require decades

805 During the implementation of RDBs a substantial amount of soil carbon was removed  
806 and replaced. Although we determined an overall 17 % reduction in soil respiration in  
807 RDBs, it will take over 100 years to realize net reductions in cumulative CO<sub>2</sub> emission if  
808 the removed carbon is assumed to be fully mineralized. According to our calculation, the  
809 time elapsed since the establishment of RDBs in our study system is only one quarter of  
810 the total time required to realize a net benefit in terms of soil carbon balance relative to  
811 CDBs (Fig. 9a). However, the uncertain validity of the assumptions used in our  
812 calculations means that this conclusion is provisional at best. Firstly, the range of  
813 environmental changes induced by the TSR and border construction may also lead to  
814 differences in net primary production (NPP) between DB types. If this is the case, the  
815 payback rate would be determined not just by the difference in soil respiration that we  
816 observed, but would be further modified by differences in annual carbon inputs (Fig. 9b;  
817 black arrows). Although we did not quantify this in our study, there is evidence that



818 different crops (*Azolla filiculoides*, *Typha angustifolia*, and *Typha latifolia*) used in  
819 paludiculture under similar conditions to our study site show different patterns in gross  
820 primary productivity in comparison to the original grassland with *L. perenne* (Van Den  
821 Berg et al., 2024). As the vegetation differed substantially between DB types, it's likely  
822 that above- and/or belowground productivity is likewise not equal. If productivity is  
823 greatly reduced in RDBs in comparison to CDBs, there is a chance that the carbon debt  
824 is not compensated for by our observed differences in soil respiration, which could in turn  
825 lead to an overall long-term carbon cost. Secondly, uncertainty arises from assuming all  
826 excavated carbon is mineralized. The excavated material could have been transferred to  
827 an environment with conditions unfavourable for mineralization (e.g. under higher water  
828 tables or anaerobic conditions), leading to a relatively lower initial carbon debt and  
829 consequently shorter payback time (Fig. 9c). If the proportion of the mineralized carbon  
830 from the removed soil reduces with 10 %, the payback time reduces with 11-12 years.  
831 Lastly, additional uncertainty arises from changes in soil abiotic conditions over the years  
832 following RDB establishment which could result in a progressively smaller difference in  
833 respiration rate between CDBs and RDBs and eventually halt the payback (Fig. 9d, green  
834 dashed lines). This could occur when peat build-up in RDBs is as fast as peat  
835 mineralization in CDBs, where after a certain number of years the C stock of both DB  
836 types converge. The faster convergence occurs, the earlier the RDBs would potentially  
837 start to show little to no net carbon benefit.

838



839

840 Fig. 9: (a) Conceptual figure of the carbon stock over time in relation to the resulting  
 841 estimated carbon debt by TSR and the positive effect of TSR on the net carbon balance ( $\Delta$   
 842 C stock) under three assumptions which then determine when reduced emissions were  
 843 realized. The lines represent the observed difference in  $R_{soil}$  between regenerative (green;  
 844 RDB) and conventional (blue; CDBs) DBs. (b) the possible effect on reduced emissions  
 845 when NPP was not equal (assumption 2; black arrows). (c) the possible effects of the  
 846 extent of the carbon debt (assumption 1; two green lines) on the resulting payback time.  
 847 (d) the possible effects when the differences driving  $R_{soil}$  are not constant in time  
 848 (assumption 3).

849

850 Similar studies looking at the carbon accounting consequences of land use conversion  
 851 in peatland agroecosystems, reached broadly similar conclusions to our study. During a  
 852 shift from intensive livestock farming to paludiculture, which is accompanied by partial  
 853 removal of the topsoil, a reduction in CO<sub>2</sub> emissions is measured (Van Den Berg et al.,  
 854 2024). However, it can take between 43-93 years (depending on the paludiculture  
 855 species) for paludiculture sites to show reduced radiative forcing and start contributing  
 856 to global warming reductions when incorporating emissions from the removed topsoil.



857 This lag in realized positive effects is partly the result of emitted CO<sub>2</sub> from the removed  
858 topsoil which is equivalent to 27 years of emissions from the control conditions (Van Den  
859 Berg et al., 2024). Another study, estimates that reductions in radiative forcing start after  
860 13-22 years (TSR depth of 30 cm) or after 40 years (TSR depth of at 60 cm) in comparison  
861 to an intensive grassland which is depending on the decomposition rate (conversion into  
862 CO<sub>2</sub>) of the removed carbon (Huth et al., 2022). However, so far the exact fate of removed  
863 carbon after TSR and RDB implementation is not clear. Estimations of different fates and  
864 their associated mineralization rates, such as spreading over field, hole filling in field, and  
865 burying under anaerobic conditions, would greatly contribute to our estimations the  
866 timescale over which net emission reduction are achieved. This implies that any  
867 measures that lead to a minimalization of CO<sub>2</sub> emissions from the excavated carbon  
868 would further improve the peat polder-scale CO<sub>2</sub> emission reduction of RDBs with the  
869 use of TSR.

870

#### 871 4.4 Management implications

872 Our study highlights the importance of creating RDBs surrounding grasslands used for  
873 livestock farming in Dutch peat meadows. TSR is often combined with groundwater table  
874 management (Huth et al., 2020; Quadra et al., 2023), however TSR used for RDBs (no  
875 rewetting) was effective in reducing soil CO<sub>2</sub> emissions. Reduced soil respiration was  
876 mainly obtained by reducing the relative amounts of carbon exposed to aerobic  
877 conditions. Implementation of RDBs creates a shift to a more regenerative farming  
878 system which would contribute to improved ecosystem services and biodiversity.

879 GHG emissions from ditches can also substantially contribute to the carbon budget in  
880 peatlands (25-33 % of the total landscape) (van der Knaap et al., 2025). So far, it's unclear  
881 whether implementing RDBs affects these emissions. RDBs have a higher perimeter-to-  
882 surface area ratio, enhanced soil-water contact, and therefore can possibly increase  
883 lateral transport of DOC, CO<sub>2</sub> and CH<sub>4</sub> to the ditch. Examining how RDBs affect these  
884 transport processes and the consequences for aquatic emissions would be needed to  
885 complete the effect of RDBs on the carbon balance.

886



## 887 5 Conclusions

888 RDBs implemented with TSR, reduced soil CO<sub>2</sub> emissions which was predominantly  
889 driven by lower amounts of exposed carbon. Border areas around ditches could  
890 contribute to reduced CO<sub>2</sub> emissions, especially where restoration of entire fields is, at  
891 this moment, not possible due to economic and political motivations. In spring and  
892 summer, small hotspots for soil CO<sub>2</sub> production might occur when optimal moisture  
893 conditions are not counteracted by a sufficient reduction in exposed carbon. For this  
894 measure to be successful, it is crucial to process and store the excavated peat soil under  
895 conditions that limit mineralization. The predictors in this study (soil temperature, soil  
896 moisture content and exposed carbon) are relatively easy to monitor and, thus, allow  
897 easy monitoring of annual soil CO<sub>2</sub> production. The National Climate Agreement 2019  
898 requires an emission reduction of 1 Mt CO<sub>2</sub>-eq from Dutch peat meadows by 2030  
899 (Rijkskoverheid, 2019). This highlights the need for effective management measures,  
900 besides restoration where feasible. Regenerative measures, such as RDBs, could  
901 contribute to more responsible and peatland-adapted agriculture which is highly needed  
902 in wetland agroecosystems in northwest Europe (Freeman et al., 2022).

903

904



905 **Code availability**

906 All code can be provided by the corresponding authors upon request.

907

908 **Data availability**

909 Data will be made available via Yoda.

910

911 **Supplement**

912 The supplement is available.

913

914 **Author contributions**

915 **Sanne Bethe:** Conceptualization, Methodology, Investigation, Formal analysis,  
916 Validation, Visualization, Writing – original draft, Writing – review & editing, Supervision.

917 **Mariet Hefting:** Conceptualization, Methodology, Writing – review & editing, Supervision.

918 **Joao Wendrich Teixeira:** Investigation, Writing – review & editing.

919 **Matty Berg:** Conceptualization, Methodology, Funding acquisition, Writing – review &  
920 editing, Supervision.

921 **James Weedon:** Conceptualization, Methodology, Validation, Writing – review & editing,  
922 Supervision.

923

924 **Competing interests**

925 The authors declare that they have no known competing financial interests or personal  
926 relationships that could have appeared to influence the work reported in this paper.

927

928 **Acknowledgements**

929 We would like to acknowledge Gertjan van Tunen (Koningshoeve) and Jelle Vink for  
930 providing us access to their fields, assisting where needed and safeguarding the



931 equipment from mowing activities, Richard van Logtestijn (Vrije Universiteit Amsterdam)

932 for his help in the laboratory and Julia Marinissen for her help with the fieldwork.

933

934 **Financial support**

935 This study was supported by the research program VeenVitaal funded by the Nationale

936 Wetenschapsagenda – Onderzoek op Routes door Consortia (NWA-ORC,

937 NWA.1389.20.125).

938

939



940 **References**

- 941 Aben, R. C. H., Van De Craats, D., Boonman, J., Peeters, S. H., Vriend, B., Boonman, C. C. F.,  
942 Van Der Velde, Y., Erkens, G., & Van Den Berg, M. (2024). CO<sub>2</sub> emissions of drained  
943 coastal peatlands in the Netherlands and potential emission reduction by water  
944 infiltration systems. *Biogeosciences*, *21*(18), 4099–4118. [https://doi.org/10.5194/BG-](https://doi.org/10.5194/BG-21-4099-2024)  
945 [21-4099-2024](https://doi.org/10.5194/BG-21-4099-2024)
- 946 Armstrong, A., Waldron, S., Ostle, N. J., Richardson, H., & Whitaker, J. (2015). Biotic and  
947 Abiotic Factors Interact to Regulate Northern Peatland Carbon Cycling. *Ecosystems* *2015*  
948 *18:8*, *18*(8), 1395–1409. <https://doi.org/10.1007/S10021-015-9907-4>
- 949 Bates, D., Mächler, M., Bolker, B. M., & Walker, S. C. (2015). Fitting linear mixed-effects  
950 models using lme4. *Journal of Statistical Software*, *67*(1).  
951 <https://doi.org/10.18637/JSS.V067.I01>
- 952 Bethe, S. E., Weedon, J. T., Marinissen, J., Berg, M. P., & Hefting, M. M. (2025). Altered litter  
953 quality drives changes in litter decomposition following implementation of a  
954 regenerative measure in Dutch peat meadows. *Journal of Environmental Management*,  
955 *378*. <https://doi.org/10.1016/j.jenvman.2025.124725>
- 956 Boonman, C. C. F., Heuts, T. S., Vroom, R. J. E., Geurts, J. J. M., & Fritz, C. (2023). Wetland  
957 plant development overrides nitrogen effects on initial methane emissions after peat  
958 rewetting. *Aquatic Botany*, *184*, 103598.  
959 <https://doi.org/10.1016/J.AQUABOT.2022.103598>
- 960 Boonman, J., Harpenslager, S. F., van Dijk, G., Smolders, A. J. P., Hefting, M. M., van de Riet,  
961 B., & van der Velde, Y. (2024). Redox potential is a robust indicator for decomposition  
962 processes in drained agricultural peat soils: A valuable tool in monitoring peatland  
963 wetting efforts. *Geoderma*, *441*, 116728.  
964 <https://doi.org/10.1016/J.GEODERMA.2023.116728>
- 965 Boonman, J., Tolunay, D., Keuskamp, J., Heffernan, L., Buzacott, A. J. V., Harpenslager, S. F.,  
966 van Dijk, G., Hefting, M., & van der Velde, Y. (2025). High contributions of anaerobic  
967 decomposition to greenhouse gas emissions of agriculturally used peatlands.  
968 *Geoderma*, *462*, 117521. <https://doi.org/10.1016/J.GEODERMA.2025.117521>
- 969 Brix, H., Sorrell, B. K., & Lorenzen, B. (2001). Are Phragmites-dominated wetlands a net  
970 source or net sink of greenhouse gases? *Aquatic Botany*, *69*(2–4), 313–324.  
971 [https://doi.org/10.1016/S0304-3770\(01\)00145-0](https://doi.org/10.1016/S0304-3770(01)00145-0)
- 972 Brouns, K., Verhoeven, J. T. A., & Hefting, M. M. (2014). Short period of oxygenation releases  
973 latch on peat decomposition. *Science of The Total Environment*, *481*(1), 61–68.  
974 <https://doi.org/10.1016/J.SCITOTENV.2014.02.030>



- 975 Bürkner, P. C. (2017). brms: An R Package for Bayesian Multilevel Models Using Stan. *Journal*  
976 *of Statistical Software*, 80, 1–28. <https://doi.org/10.18637/JSS.V080.I01>
- 977 Chimner, R. A., Cooper, D. J., Wurster, F. C., & Rochefort, L. (2017). An overview of peatland  
978 restoration in North America: where are we after 25 years? *Restoration Ecology*, 25(2),  
979 283–292. <https://doi.org/10.1111/REC.12434>
- 980 Daun, C., Gaudig, G., Huth, V., Krebs, M., & Jurasinski, G. (2026). How to minimize  
981 greenhouse gas emissions in Sphagnum re-vegetation areas - the role of topsoil  
982 removal. *Ecological Engineering*, 224, 107884.  
983 <https://doi.org/10.1016/J.ECOLENG.2025.107884>
- 984 Davidson, E. A., & Janssens, I. A. (2006). Temperature sensitivity of soil carbon  
985 decomposition and feedbacks to climate change. *Nature* 2006 440:7081, 440(7081),  
986 165–173. <https://doi.org/10.1038/nature04514>
- 987 Efron, B., & Tibshirani, R. J. (1994). An Introduction to the Bootstrap. In *An Introduction to*  
988 *the Bootstrap*. Chapman and Hall/CRC.
- 989 Erkens, G., De Vries, S., Zwanenburg, C., & Van Der Kolk, B. (2013). *Dijken op Veen II*.
- 990 Erkens, G., Van Der Meulen, M. J., & Middelkoop, H. (2016). Double trouble: Subsidence and  
991 CO<sub>2</sub> respiration due to 1,000 years of Dutch coastal peatlands cultivation. *Hydrogeology*  
992 *Journal*, 24(3), 551–568. <https://doi.org/10.1007/S10040-016-1380-4>
- 993 Fairbairn, L., Rezanezhad, F., Gharasoo, M., Parsons, C. T., Macrae, M. L., Slowinski, S., & Van  
994 Cappellen, P. (2023). Relationship between soil CO<sub>2</sub> fluxes and soil moisture: Anaerobic  
995 sources explain fluxes at high water content. *Geoderma*, 434, 116493.  
996 <https://doi.org/10.1016/J.GEODERMA.2023.116493>
- 997 Fairlie, R. W. (2005). An extension of the Blinder-Oaxaca decomposition technique to logit  
998 and probit models. *Journal of Economic and Social Measurement*, 30(4), 305–316.  
999 <https://doi.org/10.3233/JEM-2005-0259;WGROU:STRING:PUBLICATION>
- 1000 Fernández-Pascual, E., & Correia-Álvarez, E. (2021). Mire microclimate: Groundwater buffers  
1001 temperature in waterlogged versus dry soils. *International Journal of Climatology*,  
1002 41(S1), E2949–E2958. <https://doi.org/http://dx.doi.org/10.1002/joc.6893>
- 1003 Findlay, S. E. G. (2021). Organic Matter Decomposition. *Fundamentals of Ecosystem Science*,  
1004 *Second Edition*, 81–102. <https://doi.org/10.1016/B978-0-12-812762-9.00004-6>
- 1005 Freeman, B. W. J., Evans, C. D., Musarika, S., Morrison, R., Newman, T. R., Page, S. E., Wiggs,  
1006 G. F. S., Bell, N. G. A., Styles, D., Wen, Y., Chadwick, D. R., & Jones, D. L. (2022).  
1007 Responsible agriculture must adapt to the wetland character of mid-latitude peatlands.  
1008 *Global Change Biology*, 28(12), 3795–3811. <https://doi.org/10.1111/gcb.16152>



- 1009 Galloway, D. L., Erkens, G., Kuniandy, E. L., & Rowland, J. C. (2016). Preface: Land subsidence  
1010 processes. *Hydrogeology Journal*, 24(3), 547–550. [https://doi.org/10.1007/s10040-016-](https://doi.org/10.1007/s10040-016-1386-y)  
1011 1386-y
- 1012 Gorham, E. (1991). Northern peatlands: role in the carbon cycle and probable responses to  
1013 climatic warming. *Ecological Applications*, 1(2), 182–195.  
1014 <https://doi.org/10.2307/1941811>
- 1015 Harpenslager, S. F., van den Elzen, E., Kox, M. A. R., Smolders, A. J. P., Ettwig, K. F., & Lamers,  
1016 L. P. M. (2015). Rewetting former agricultural peatlands: Topsoil removal as a  
1017 prerequisite to avoid strong nutrient and greenhouse gas emissions. *Ecological*  
1018 *Engineering*, 84, 159–168. <https://doi.org/10.1016/J.ECOLENG.2015.08.002>
- 1019 Hendriks, D. M. D., Van Huissteden, J., Dolman, A. J., & Van Der Molen, M. K. (2007). The full  
1020 greenhouse gas balance of an abandoned peat meadow. *Biogeosciences*, 4(3), 411–424.  
1021 <https://doi.org/10.5194/bg-4-411-2007>
- 1022 Huang, Y., Ciais, P., Luo, Y., Zhu, D., Wang, Y., Qiu, C., Goll, D. S., Guenet, B., Makowski, D., De  
1023 Graaf, I., Leifeld, J., Kwon, M. J., Hu, J., & Qu, L. (2021). Tradeoff of CO<sub>2</sub> and CH<sub>4</sub>  
1024 emissions from global peatlands under water-table drawdown. *Nature Climate Change*  
1025 2021 11:7, 11(7), 618–622. <https://doi.org/10.1038/s41558-021-01059-w>
- 1026 Humpenöder, F., Karstens, K., Lotze-Campen, H., Leifeld, J., Menichetti, L., Barthelmes, A., &  
1027 Popp, A. (2020). Peatland protection and restoration are key for climate change  
1028 mitigation. *Environmental Research Letters*, 15(10), 104093.  
1029 <https://doi.org/10.1088/1748-9326/ABAE2A>
- 1030 Huth, V., Günther, A., Bartel, A., Gutekunst, C., Heinze, S., Hofer, B., Jacobs, O., Koebisch, F.,  
1031 Rosinski, E., Tonn, C., Ullrich, K., & Jurasinski, G. (2022). The climate benefits of topsoil  
1032 removal and Sphagnum introduction in raised bog restoration. *Restoration Ecology*,  
1033 30(1), e13490. <https://doi.org/10.1111/REC.13490>
- 1034 Huth, V., Günther, A., Bartel, A., Hofer, B., Jacobs, O., Jantz, N., Meister, M., Rosinski, E.,  
1035 Urich, T., Weil, M., Zak, D., & Jurasinski, G. (2020). Topsoil removal reduced in-situ  
1036 methane emissions in a temperate rewetted bog grassland by a hundredfold. *Science of*  
1037 *The Total Environment*, 721, 137763.  
1038 <https://doi.org/10.1016/J.SCITOTENV.2020.137763>
- 1039 Joosten, H. (2009). The Global Peatland CO<sub>2</sub> Picture: peatland status and drainage related  
1040 emissions in all countries of the world. *Wetland International*.
- 1041 Joosten, H. (2015). *Peatlands, Climate Change Mitigation and Biodiversity Conservation. An*  
1042 *Issue Brief on the Importance of Peatlands for Carbon and Biodiversity Conservation and*  
1043 *the Role of Drained Peatlands as Greenhouse Gas Emission Hotspots*. Nordic Council of  
1044 Ministers.



- 1045 Käärmelahti, S. A., Fritz, C., Quadra, G. R., Gardoki, M. E., Gaudig, G., Krebs, M., & Temmink,  
1046 R. J. M. (2024). Topsoil removal for Sphagnum establishment on rewetted agricultural  
1047 bogs. *Biogeochemistry*, 167(4), 479–496. <https://doi.org/10.1007/S10533-023-01096-X>
- 1048 Kechavarzi, C., Dawson, Q., Bartlett, M., & Leeds-Harrison, P. B. (2010). The role of soil  
1049 moisture, temperature and nutrient amendment on CO<sub>2</sub> efflux from agricultural peat  
1050 soil microcosms. *Geoderma*, 154(3–4), 203–210.  
1051 <https://doi.org/10.1016/J.GEODERMA.2009.02.018>
- 1052 Kucera, C. L., & Kirkham, D. R. (1971). Soil Respiration Studies in Tallgrass Prairie in Missouri.  
1053 *Ecology*, 52(5), 912–915. <https://doi.org/10.2307/1936043>
- 1054 Kuznetsova, A., Brockhoff, P. B., & Christensen, R. H. B. (2017). lmerTest Package: Tests in  
1055 Linear Mixed Effects Models. *Journal of Statistical Software*, 82(13), 1–26.  
1056 <https://doi.org/10.18637/JSS.V082.I13>
- 1057 Kuzyakov, Y. (2010). Priming effects: Interactions between living and dead organic matter. *Soil*  
1058 *Biology and Biochemistry*, 42(9), 1363–1371.  
1059 <https://doi.org/10.1016/j.soilbio.2010.04.003>
- 1060 Kuzyakov, Y., Ehrensberger, H., & Stahr, K. (2001). Carbon partitioning and below-ground  
1061 translocation by *Lolium perenne*. *Soil Biology and Biochemistry*, 33(1), 61–74.  
1062 [https://doi.org/10.1016/S0038-0717\(00\)00115-2](https://doi.org/10.1016/S0038-0717(00)00115-2)
- 1063 Laiho, R., Silvan, N., Cárcamo, H., & Vasander, H. (2001). Effects of water level and nutrients  
1064 on spatial distribution of soil mesofauna in peatlands drained for forestry in Finland.  
1065 *Applied Soil Ecology*, 16(1), 1–9. [https://doi.org/10.1016/S0929-1393\(00\)00103-7](https://doi.org/10.1016/S0929-1393(00)00103-7)
- 1066 Leifeld, J., & Menichetti, L. (2018). The underappreciated potential of peatlands in global  
1067 climate change mitigation strategies. *Nature Communications*, 9(1), 1–7.  
1068 <https://doi.org/10.1038/s41467-018-03406-6>
- 1069 Leifeld, J., Müller, M., & Fuhrer, J. (2011). Peatland subsidence and carbon loss from drained  
1070 temperate fens. *Soil Use and Management*, 27(2), 170–176.  
1071 <https://doi.org/10.1111/j.1475-2743.2011.00327.x>
- 1072 Li, G., & Sun, S. (2011). Plant clipping may cause overestimation of soil respiration in a  
1073 Tibetan alpine meadow, southwest China. *Ecological Research* 2011 26:3, 26(3), 497–  
1074 504. <https://doi.org/10.1007/s11284-011-0806-7>
- 1075 Linn, D. M., & Doran, J. W. (1984). Effect of Water-Filled Pore Space on Carbon Dioxide and  
1076 Nitrous Oxide Production in Tilled and Nontilled Soils. *Soil Science Society of America*  
1077 *Journal*, 48(6), 1267–1272.  
1078 <https://doi.org/10.2136/SSSAJ1984.03615995004800060013X>
- 1079 Lloyd, J., & Taylor, J. A. (1994). On the Temperature Dependence of Soil Respiration.  
1080 *Functional Ecology*, 8(3), 315. <https://doi.org/10.2307/2389824>



- 1081 Loisel, J., Yu, Z., Beilman, D. W., Camill, P., Alm, J., Amesbury, M. J., Anderson, D., Andersson,  
1082 S., Bochicchio, C., Barber, K., Belyea, L. R., Bunbury, J., Chambers, F. M., Charman, D. J.,  
1083 De Vleeschouwer, F., Fiałkiewicz-Kozielec, B., Finkelstein, S. A., Gałka, M., Garneau, M., ...  
1084 Zhou, W. (2014). A database and synthesis of northern peatland soil properties and  
1085 Holocene carbon and nitrogen accumulation. *Holocene*, 24(9), 1028–1042.  
1086 <https://doi.org/10.1177/0959683614538073>
- 1087 Mäkiranta, P., Laiho, R., Fritze, H., Hytönen, J., Laine, J., & Minkkinen, K. (2009). Indirect  
1088 regulation of heterotrophic peat soil respiration by water level via microbial community  
1089 structure and temperature sensitivity. *Soil Biology and Biochemistry*, 41(4), 695–703.  
1090 <https://doi.org/10.1016/J.SOILBIO.2009.01.004>
- 1091 Manzoni, S., Schimel, J. P., & Porporato, A. (2012). Responses of soil microbial communities  
1092 to water stress: results from a meta-analysis. *Ecology*, 93(4), 930–938.  
1093 <https://doi.org/10.1890/11-0026.1>
- 1094 Minke, M., Augustin, J., Burlo, A., Yarmashuk, T., Chuvashova, H., Thiele, A., Freibauer, A.,  
1095 Tikhonov, V., & Hoffmann, M. (2016). Water level, vegetation composition, and plant  
1096 productivity explain greenhouse gas fluxes in temperate cutover fens after inundation.  
1097 *Biogeosciences*, 13(13), 3945–3970. <https://doi.org/10.5194/BG-13-3945-2016>
- 1098 Minkkinen, K., Laine, J., Shurpali, J., Mäkiranta, P., Alm, J., & Penttilä, T. (2007). Heterotrophic  
1099 soil respiration in forestry-drained peatlands. *Boreal Environ Res*, 12, 115–126.
- 1100 Möhl, P., Vorkauf, M., Kahmen, A., & Hiltbrunner, E. (2023). Recurrent summer drought  
1101 affects biomass production and community composition independently of snowmelt  
1102 manipulation in alpine grassland. *Journal of Ecology*, 111(11), 2357–2375.  
1103 <https://doi.org/10.1111/1365-2745.14180>
- 1104 Moyano, F. E., Manzoni, S., & Chenu, C. (2013). Responses of soil heterotrophic respiration to  
1105 moisture availability: An exploration of processes and models. *Soil Biology and*  
1106 *Biochemistry*, 59, 72–85. <https://doi.org/10.1016/J.SOILBIO.2013.01.002>
- 1107 Quadra, G. R., Boonman, C. C. F., Vroom, R. J. E., Temmink, R. J. M., Smolders, A. J. P., Geurts,  
1108 J. J. M., Aben, R. C. H., Weideveld, S. T. J., & Fritz, C. (2023). Removing 10 cm of  
1109 degraded peat mitigates unwanted effects of peatland rewetting: a mesocosm study.  
1110 *Biogeochemistry*, 163(1), 65–84. <https://doi.org/10.1007/S10533-022-01007-6>
- 1111 Renou-Wilson, F., Moser, G., Fallon, D., Farrell, C. A., Müller, C., & Wilson, D. (2019).  
1112 Rewetting degraded peatlands for climate and biodiversity benefits: Results from two  
1113 raised bogs. *Ecological Engineering*, 127, 547–560.  
1114 <https://doi.org/10.1016/J.ECOLENG.2018.02.014>
- 1115 Rijksverheid. (2019). *Climate Agreement*.



- 1116 Schjøning, P., Thomsen, I. K., Moldrup, P., & Christensen, B. T. (2003). Linking Soil Microbial  
1117 Activity to Water- and Air-Phase Contents and Diffusivities. *Soil Science Society of*  
1118 *America Journal*, 67(1), 156–165. <https://doi.org/10.2136/SSSAJ2003.1560>
- 1119 Searle, S. R., Speed, F. M., & Milliken, G. A. (2012). Population marginal means in the linear  
1120 model: An alternative to least squares means. *American Statistician*, 34(4), 216–221.  
1121 <https://doi.org/10.1080/00031305.1980.10483031>
- 1122 Skopp, J., Jawson, M. D., & Doran, J. W. (1990). Steady-State Aerobic Microbial Activity as a  
1123 Function of Soil Water Content. *Soil Science Society of America Journal*, 54(6), 1619–  
1124 1625. <https://doi.org/10.2136/SSSAJ1990.03615995005400060018X>
- 1125 Štrumbelj, E., & Kononenko, I. (2013). Explaining prediction models and individual  
1126 predictions with feature contributions. *Knowledge and Information Systems 2013 41:3*,  
1127 41(3), 647–665. <https://doi.org/10.1007/S10115-013-0679-X>
- 1128 Suseela, V., Conant, R. T., Wallenstein, M. D., & Dukes, J. S. (2012). Effects of soil moisture on  
1129 the temperature sensitivity of heterotrophic respiration vary seasonally in an old-field  
1130 climate change experiment. *Global Change Biology*, 18(1), 336–348.  
1131 <https://doi.org/10.1111/J.1365-2486.2011.02516.X>
- 1132 Tanneberger, F., Appulo, L., Ewert, S., Lakner, S., Ó Brocháin, N., Peters, J., & Wichtmann, W.  
1133 (2021). The Power of Nature-Based Solutions: How Peatlands Can Help Us to Achieve  
1134 Key EU Sustainability Objectives. *Advanced Sustainable Systems*, 5(1).  
1135 <https://doi.org/10.1002/ADSU.202000146>
- 1136 Tiemeyer, B., Freibauer, A., Borraz, E. A., Augustin, J., Bechtold, M., Beetz, S., Beyer, C., Ebli,  
1137 M., Eickenscheidt, T., Fiedler, S., Förster, C., Gensior, A., Giebels, M., Glatzel, S.,  
1138 Heinichen, J., Hoffmann, M., Höper, H., Jurasinski, G., Laggner, A., ... Drösler, M. (2020).  
1139 A new methodology for organic soils in national greenhouse gas inventories: Data  
1140 synthesis, derivation and application. *Ecological Indicators*, 109, 105838.  
1141 <https://doi.org/10.1016/J.ECOLIND.2019.105838>
- 1142 Tolunay, D., Kowalchuk, G. A., Erkens, G., & Hefting, M. M. (2024). Aerobic and anaerobic  
1143 decomposition rates in drained peatlands: Impact of botanical composition. *Science of*  
1144 *The Total Environment*, 930. <https://doi.org/10.1016/J.SCITOTENV.2024.172639>
- 1145 van Baren, S. A., Arets, E. J. M. M., Hendriks, C. M. J., Kramer, H., Lesschen, J. P., & Schelhaas,  
1146 M. J. (2024). *Greenhouse gas reporting of the LULUCF sector in the Netherlands :*  
1147 *Methodological background, update 2024.*
- 1148 van de Ven, G. (1993). Man-made lowlands: history of water management and land  
1149 reclamation in the Netherlands. *Uitgeverij Matrijs.*
- 1150 Van Den Berg, M., Gremmen, T. M., Vroom, R. J. E., Van Huissteden, J., Boonman, J., Van  
1151 Huissteden, C. J. A., Van Der Velde, Y., Smolders, A. J. P., & Van De Riet, B. P. (2024). A



- 1152 case study on topsoil removal and rewetting for paludiculture: effect on  
1153 biogeochemistry and greenhouse gas emissions from *Typha latifolia*, *Typha angustifolia*,  
1154 and *Azolla filiculoides*. *Biogeosciences*, 21(11), 2669–2690. [https://doi.org/10.5194/BG-](https://doi.org/10.5194/BG-21-2669-2024)  
1155 21-2669-2024,
- 1156 van der Knaap, J., Harpenslager, S. F., Aben, R. C. H., Weideveld, S. T. J., van Giersbergen, Q.,  
1157 van Dijk, G., Wintjen, P., Buzacott, A. J. V., Fritz, C., Kruijt, B., & Kosten, S. (2025).  
1158 Disproportionately High Contribution of Ditches to Landscape Greenhouse Gas  
1159 Emissions in Drained Peatlands. *Ecosystems*, 28(5), 58-  
1160 <https://doi.org/10.1007/s10021-025-01005-3>
- 1161 van der Laan, A., van Eekeren, N., Wassen, M. J., Rebel, K. T., & van Dijk, J. (2025). Soil biota  
1162 response to raised water levels and reduced nutrient inputs in agricultural peat  
1163 meadows. *Applied Soil Ecology*, 207, 105932.  
1164 <https://doi.org/10.1016/J.APSOIL.2025.105932>
- 1165 van Dijk, J., Didden, W. A. M., Kuenen, F., van Bodegom, P. M., Verhoef, H. A., & Aerts, R.  
1166 (2009). Can differences in soil community composition after peat meadow restoration  
1167 lead to different decomposition and mineralization rates? *Soil Biology and Biochemistry*,  
1168 41(8), 1717–1725. <https://doi.org/10.1016/J.SOILBIO.2009.05.016>
- 1169 van Vossen, J., & Verhagen, D. (2009). *HANDREIKING NATUURVRIENDELIJKE OEVERS*.  
1170 Stichting Toegepast Onderzoek Waterbeheer.
- 1171 Weideveld, S. T. J., Liu, W., Van Den Berg, M., Lamers, L. P. M., & Fritz, C. (2021).  
1172 Conventional subsoil irrigation techniques do not lower carbon emissions from drained  
1173 peat meadows. *Biogeosciences*, 18(12), 3881–3902. [https://doi.org/10.5194/BG-18-](https://doi.org/10.5194/BG-18-3881-2021)  
1174 3881-2021
- 1175 Wereld Natuur Fonds. (2020). *Living Planet Report Nederland. Natuur en landbouw*  
1176 *verbonden*.
- 1177 Wild, J., Kopecký, M., Macek, M., Šanda, M., Jankovec, J., & Haase, T. (2019). Climate at  
1178 ecologically relevant scales: A new temperature and soil moisture logger for long-term  
1179 microclimate measurement. *Agricultural and Forest Meteorology*, 268, 40–47.  
1180 <https://doi.org/10.1016/J.AGRFORMET.2018.12.018>
- 1181 Yu, Z., Loisel, J., Brosseau, D. P., Beilman, D. W., & Hunt, S. J. (2010). Global peatland  
1182 dynamics since the Last Glacial Maximum. *Geophysical Research Letters*, 37(13).  
1183 <https://doi.org/10.1029/2010GL043584>
- 1184 Zak, D., & McInnes, R. J. (2022). A call for refining the peatland restoration strategy in  
1185 Europe. *Journal of Applied Ecology*, 59(11), 2698–2704. [https://doi.org/10.1111/1365-](https://doi.org/10.1111/1365-2664.14261)  
1186 2664.14261



- 1187 Zak, D., Meyer, N., Cabezas, A., Gelbrecht, J., Mauersberger, R., Tiemeyer, B., Wagner, C., &  
1188 McInnes, R. (2017). Topsoil removal to minimize internal eutrophication in rewetted  
1189 peatlands and to protect downstream systems against phosphorus pollution: A case  
1190 study from NE Germany. *Ecological Engineering*, 103, 488–496.  
1191 <https://doi.org/10.1016/J.ECOLENG.2015.12.030>
- 1192 Zak, D., Wagner, C., Payer, B., Augustin, J., & Gelbrecht, J. (2010). Phosphorus mobilization in  
1193 rewetted fens: The effect of altered peat properties and implications for their  
1194 restoration. *Ecological Applications*, 20(5), 1336–1349. [https://doi.org/10.1890/08-](https://doi.org/10.1890/08-2053.1)  
1195 [2053.1](https://doi.org/10.1890/08-2053.1)
- 1196
- 1197
- 1198